No. RITARS-14-H-RUT

Mobile Hybrid LiDAR & Infrared Sensing for Natural Gas Pipeline Monitoring

Final Report

Performance Period:

January 15, 2014 – June 30, 2016

Principal Investigator:

Jie Gong, Ph.D., CM-BIM

Assistant Professor

Center for Advanced Infrastructure and Transportation

Rutgers, The State University of New Jersey

1

TABLE OF CONTENTS

LIST OF FIGURES

LIST OF TABLES

EXECUTIVE SUMMARY

The natural gas distribution system in the U.S. has a total of 1.2 million miles of mains and about 65 million service lines as of 2012 [1]. This distribution system consists of various material types and is subjected to various threats which vary according to these material types, age, locations, and operational characteristics of the pipeline. This distribution system is subjected to multiple threats which result in various potential damages based on material type, age, location, and operational characteristics of the pipeline. Among other things, natural disasters are rising threats to the integrity of natural gas systems. For example, threats due to natural forces (e.g., landslides, erosion, floods, earthquakes, and other environmental hazards) contributed to about 8.6 percent of these incidents in 2015 [1]. There is growing concern in the United States about managing this vast network of pipelines as weather systems become increasingly aggressive and natural disasters become more frequent. During natural disasters such as hurricane and floods, pipelines can rupture and break due to permanent ground displacement, landslide, and collapsing building structures. This damage can cause significant post-disaster catastrophes such as fires, explosions, personal property loss, and environmental pollution. timely assessment of pipeline integrity is critical to prevent further post-disaster damages. However, such assessment is currently hampered by a) the lack of data sufficient for quantifying changes in pipeline conditions and their built environment, and b) the lack of data-driven risk models that identify high risk pipe segments after a disaster.

This project is directed at exploring the integration of several remote-sensing technologies and developing dedicated data processing and decision support tools that would allow pipeline operators to monitor changes in the built environment (structures, terrain, etc.) adjacent to pipelines after a natural disaster and to allow operators to assess the potential for increased risk of failure. This project is a joint collaboration between Rutgers' Center for Advanced Infrastructure and Transportation and Gas Technology Institute. The overall goal of this project is to: (1) provide new remote-sensing capabilities for pipeline performance after natural disasters; (2) develop the ability to detect changes and anomalies in the environment which could indicate threats to pipelines; and (3) develop GIS-based pipeline risk-assessment tools to identify and rank high risks.

The first stage of this project involved developing, deploying, and validating a mobile mapping platform that integrates commercially available high-precision global navigation, laser scanning, and infrared thermography technologies to provide new remote sensing capabilities for pipeline risk assessment. The second stage of the project investigated fusion of remote sensing data from multiple resources including mobile mapping system, airborne lidar, and UAV-borne imagery to provide automated threat detection capabilities. The last stage of this project focused on evaluating and ranking risks based on the characteristics of gas distribution systems and quantified spatially distributed threats.

In the project, two processes were evaluated: 1) Assessments for meters and aboveground gas lines (based on the assessment of buildings, conditions, and movements), and 2) assessments of belowground gas lines (based on soil movement and flood levels). Building movements were obtained from the LiDAR data and additional site surveys. (LiDAR is a remote sensing technology that measures distance by illuminating a target with a laser and analyzing the reflected light.) In order to establish limit values to pipe deformations and strains where a high likelihood of damage occurs, a Finite Element Analysis was performed to determine strains and deformations of various pipe materials and sizes, soil types, and displacement lengths. The results of the analysis were integrated in a risk approach to estimate the risk. The Integrated Risk Model provided a comprehensive risk-analysis process which considered all required risk factors and allowed for updating the initial risk predictions in light of new pertinent data. The post-disaster LiDAR study area of Ortley Beach, NJ, was selected as a model for the analysis after hurricane Sandy. The pre-disaster coordinates of the gas distribution system (i.e., mains, service lines, and meter risers) were compared with the post-disaster coordinates to evaluate soil movement and changes in the water level before and after the disaster.

For this project, investigators prepared a procedure used for a damage-probability assessment of distribution pipes due to natural forces threats. A survey of utility representatives participating in a DIMP showed that:

(1) Many utilities were using in-house spreadsheets in their risk analysis. Others were using, or considering the use of, commercial tools.

(2) Most of the commercial products can link DIMP data management to existing GIS.

(3) The participating utilities used historical data and expertise to rank and validate their risk parameters.

(4) Most of the utilities focused their risk analyses on specific threats in their system. These threats were corrosion, hazardous leaks, and cast-iron replacement programs.

Defining risk for the natural forces threats requires the assessment of disparate data sources to identify where the gas system crosses roads, railroads, floodplains, bodies of water, and wetlands. Researchers found that current utility practices for risk management include using subject-matter-expert input and ranking risks in in-house custom-built formats or from available commercial software. Gas distribution pipelines may experience high longitudinal pullout forces and, consequently, strains in the events of soil movement, slope instability, and flooding. Several studies provide procedures for the design and construction of buried pipeline in areas prone to soil movement hazards. However, researchers found that few design codes and standards provide adequate guidance on the allowable defect sizes for strain based loading. Flooding may result in increased bending stresses and damage to buried gas mains and services. In old cast iron mains which experience frequent joint leaks, water may intrude inside the pipe through the joints if the water head is higher than the internal pressure of the pipe. Water levels that cover gas service meters and regulators may also present safety risks. In post-disaster analysis of pipe risks due to soil movement, pipe displacements and strains are used to define the risk factors. The American Society of Civil Engineers provides an allowable acceptable criteria defined by loads, stresses, deformations, and strains for pipelines subjected to outside forces. The American Society of Mechanical Engineers also specifies an alternate design of pipes based on strains in situations where the pipeline experiences a predictable noncyclic displacement of its support. The combined risks from soil movement, flood, and historical pipe leak and corrosion data are incorporated in a "Bayesian Network" approach to estimate the conditional probability of damage.

Information from this project can be used to enhance the safety of gas distribution and system and provide gas system operators with an improved ability to manage their

pipeline systems. While research resulted in an integrated risk approach to natural gas distribution pipelines subjected to earth movement, landslides, and flooding (commonly associated with hurricane forces), the procedures developed in this project are also applicable to other threats and their associated risk parameters.

ACKNOWLEDGEMENTS

DISCLAIMER

The views, opinions, findings and conclusions reflected in this presentation are the responsibility of the authors only and do not represent the official policy or position of the USDOT/OST-R, or any State or other entity

GLOSSARY OF TERMS

AGA: American Gas Association

BN: Bayesian Network

CAIT: Center for Advanced Infrastructure and Transportation, Rutgers University

CCF: Common Cause Failures, failure types associated with several threats

COF: Consequence of Failure

CFR: Code of Federal Regulations

GPTC: Gas Piping Technology Committee

DIMP: Distribution Integrity Management Program

DOT: Department of transportation

PHMSA: Pipeline and Hazardous Materials Safety Administration, U.S. DOT

FEA: Finite Element Analysis

FEMA: Federal Emergency Management Agency

GIS: Geographic Information System

GTI: Gas Technology Institute

IM: Integrity Management Plan

LDC: Local gas Distribution Companies

LiDAR: Laser-focused imaging technology to measure distance

LOF: Likelihood of Failure

OTD: Operations Technology Development

POF: Probability of Failure, same as LOF

RITA: Research and Innovative Technology Administration, U.S. DOT

SME: Subject Matter Expert's opinion

SMYS: Specified Minimum Yield Strength of the pipe material

CHAPTER 1. INTRODUCTION

This collaborative project between Rutgers University and Gas Technology Institute (GTI) aimed at addressing the challenges in post-disaster assessment of natural gas pipeline systems in an increasingly aggressive climate system. In an emergency situation following a disaster, thorough pipeline safety assessments must be performed, in order to avoid costly post-disaster damages and to ensure the safe and reliable delivery of energy resources. However, such assessment is currently hampered by a) the lack of data sufficient for quantifying changes in pipeline conditions and their built environment, and b) the lack of data-driven risk models that identify high risk pipe segments after a disaster. The research team consisting of research teams from Rutgers and Gas Technology Institute accomplished three research objectives: (1) developing a mobile mapping platform that harnesses commercially available remote sensing technologies to provide new remote sensing capabilities for pipeline risk assessment; (2) developing a point cloud and infrared imagery analysis system that semi-automates extraction of data from remote sensing systems to detect changes and anomalies in the built environment that could indicate threats to pipelines; and (3) developing GIS-based pipeline risk assessment tools to identify high risk pipe segments to prioritize repair and restoration activities. The outcome of this project is a system that starts with data collection and ends with actionable information for decision makers. The project product can be readily implemented by stakeholders in pipeline safety.

This project developed and used remote sensing systems to assess gas line damages after major hurricane events. The entire framework is shown in Figure 1. Our developed approach not only gathers necessary remotely sensed data to identify threat but also provides an estimation of the probability of failure of both aboveground and belowground facilities. The damage assessment product has two capabilities:

(1) Assess the displacements of the aboveground gas facilities (e.g., gas meters and pipe risers) due to buildings movements (Figure 2). The assessment assumes that the gas meters are fully attached to the buildings and are subjected to equal movement. The building assessment is based on fusion of multiple types of remotely sensed data.
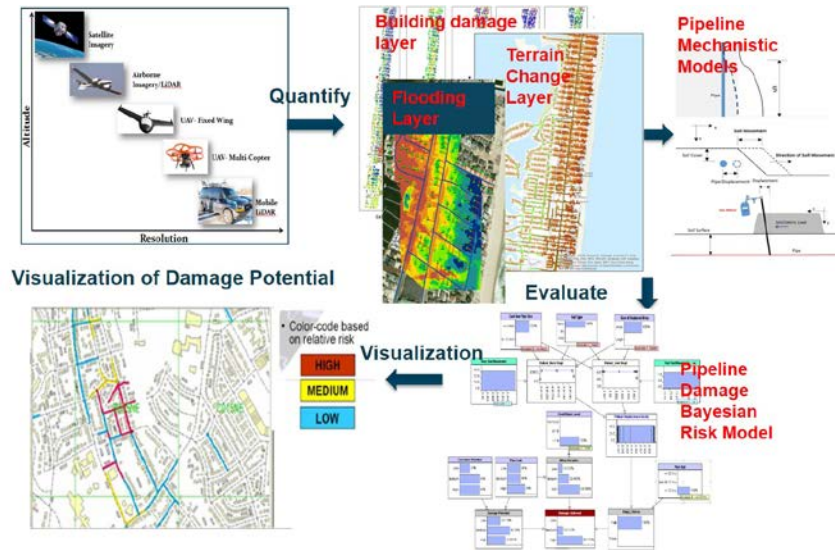
Figure 1 Project Framework
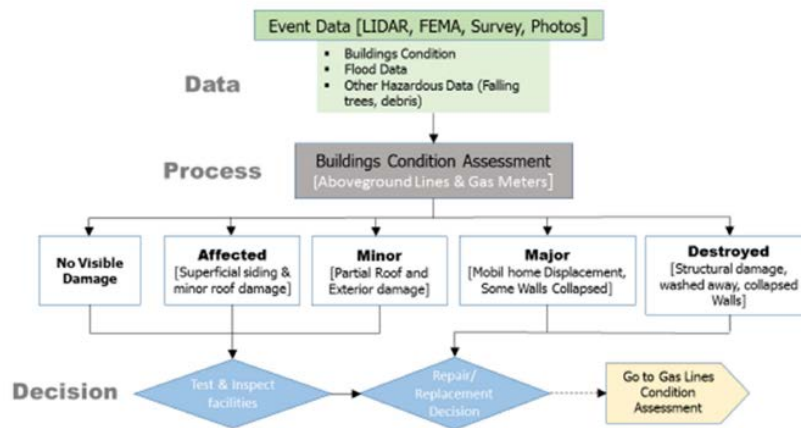
Figure 2 Layout of the aboveground assessment procedure

(2) The second step of the approach evaluates the displacements and strains of belowground gas pipes due to horizontal and vertical soil movement at the surface. Local survey data may be used with the remote sensing techniques to differentiate between the vertical changes due to soil movement and those resulting from accumulated debris. Soil movements are used along with pipeline properties in the web-based Pipe Assess program to estimate the probabilities of damages. A layout of the belowground assessment procedure is shown in Figure 3.
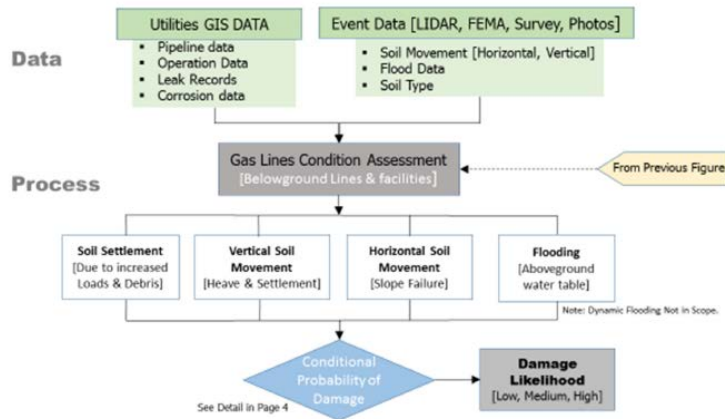
Figure 3 Layout of the aboveground assessment procedure

In addition to meeting all required deliverables, this project resulted in the publication of 1 peer reviewed journal article, 2 peer reviewed conference papers, and four additional journal papers and one conference paper in the final stages of preparation and review (See APPENDIX G for details). The research team made 15 presentations and demonstrations to audiences. Project outreach activities and research feedback initiatives were also conducted through 3 conference calls, 2 face-to-face meetings, and 1 workshop with an Advisory Stakeholder group. Major natural gas utility companies in the northeast coast including Public Service and Electric and Gas (PSEG), New York State Electric and Gas (NYSEG), Con Edison of New York, National Grid, New Jersey Natural Gas, and South Jersey Gas and regulatory agencies such as New Jersey Board of Public Utility have participated in the Remote Sensing workshop at the end of this project.

In term of project result implementation, our developed hybrid mobile mapping system has already been deployed in a FEMA funded Rebuilding with Greater Resilience project to scan nearly 800 miles of coastal roads, utility and building structures. The captured data will serve as the foundation for hurricane risk mitigation in the region for the years to come. In addition, our developed spatially resolved infrared thermography method has been called on for service in several emergency infrastructure inspection tasks including assessing and evaluating the health condition of several deteriorating bridges as part of NJDOT bridge resource program and assessing the condition of a critical tunnel in California. We have also applied our system to accomplish scanning of the iconic Port Authority Bus Terminal in New York City and provided models for terminal simulation. More recently, Bentley has pledged three years of support at the rate

15

of $25,000 per year to support our group of work with city-scale mapping and modeling with our developed system, which will further adoption of our developed spatial analytics in the Architecture, Engineering, Construction industry. Lastly, a notice of invention has been filed to the office of commercialization at Rutgers to explore ways of patenting the developed hybrid mobile lidar system and this is still active investigation.

The project was divided into the following seven research tasks.

Task 1: Technical Advisory Committee

Task 2: Post-Disaster Mobile Mapping of Pipeline Systems and Environmental Conditions

Task 3: Threat Indicator Detection

Task 4: Pipeline Risk Assessment for Decision Support

Task 5: Demonstration and Technology Transfer

Task 6: Reporting and Meetings

Task 7: Implementation Plan

In the following chapters, we describe the detailed research effort and research outcome in these tasks. Chapter 2 focuses on the task of post-disaster mobile mapping of pipeline systems and environmental conditions. Chapter 3 describes program development and data fusion methods for threat indicator detection. Chapter 4 describes the integration of remotely sensed data with pipeline risk assessment model for rapid assessment of pipeline conditions after major disasters. Chapter 5 reports activities related to industry advisory board, industry outreach, field demonstration, and implementations. It is a collective summary for Tasks 1, 5, and 7.

CHAPTER 2. POST-DISASTER MAPPING OF PIPELINE SYSTEMS AND ENVIRONMENTAL CONDITIONS

In this research task, the focus is on developing a hybrid mobile lidar and infrared system that can be used to map pipeline systems and their surrounding environment. The principle of the developed system is to use a GPS antenna, a tactical-grade IMU, a GPS ground station, and a GNSS/INS receiver to derive high-precision vehicle positions and headings, which provides a geospatial reference system for the data collected from the lidar system and the infrared sensor (Figure 4). For the navigation system, the Applanix POS LV220 system was chosen as the primary GNSS solution. The Applanix navigation system has been widely used in robotics applications such as driverless cars. Two types of lidar sensors have been integrated into the system. They include Velodyne lidar and Faro Focus 3D scanners. The system is mounted on a rack that was specially designed for easy installation of navigation sensors and other spatial sensors (Figure 5). The entire system is hosted on a Nissan van that has been modified to provide adequate workspace (Figure 6). In the initial stage of the project, we have predominately used Faro Focus 3D scanner. In the late stage of the project, Velodyne lidar was used in place of Faro Scanner due to its real-time data visualization capabilities (Figure 7).

Figure 4 The Mobile Mapping System Components

Figure 5 The Installed Sensor Mounting Platform

Figure 6 Mobile Lidar Van

Figure 7 Velodyne Lidar Sensor

The integration of all these sensors allows each piece of sensor data has a global time stamp referencing to the GNSS/INS receiver clock. In essence, other sensing technologies can be incorporated into this system as long as these sensing technologies can record time-stamped measurement. The lidar sensors and infrared thermography sensors are carefully calibrated to ensure the data can be geometrically aligned. Calibration of LiDAR and infrared sensors includes several activities: (1) Infrared sensor calibration; and (2) Developing algorithms to estimate the fundamental matrix between point clouds and infrared image data. The following sections provide detailed explanations for each activity.

Calibration of a FLIR Infrared Camera: Similar to regular digital cameras, infrared cameras can be calibrated to create a stereo-pair with other vision sensors such as LiDAR sensor. The essential problem is to estimate the projection of points in the space onto the image plane in the infrared sensor. Therefore, common camera calibration methods can be used with slight modification. The most important modification is the calibration patterns to be used. Black and white check boards are widely used as a calibration pattern for regular digital cameras. But the corners of these kinds of check boards are not quite visible to infrared sensors. To overcome this limitation, a board with regularly spaced LED lights is used as the calibration pattern (Figure 7).

The heat signatures from the LED lights can be easily identified in infrared images. The sensor to be calibrated is a FLIR infrared camera with a 640x480 resolution (Figure 8).
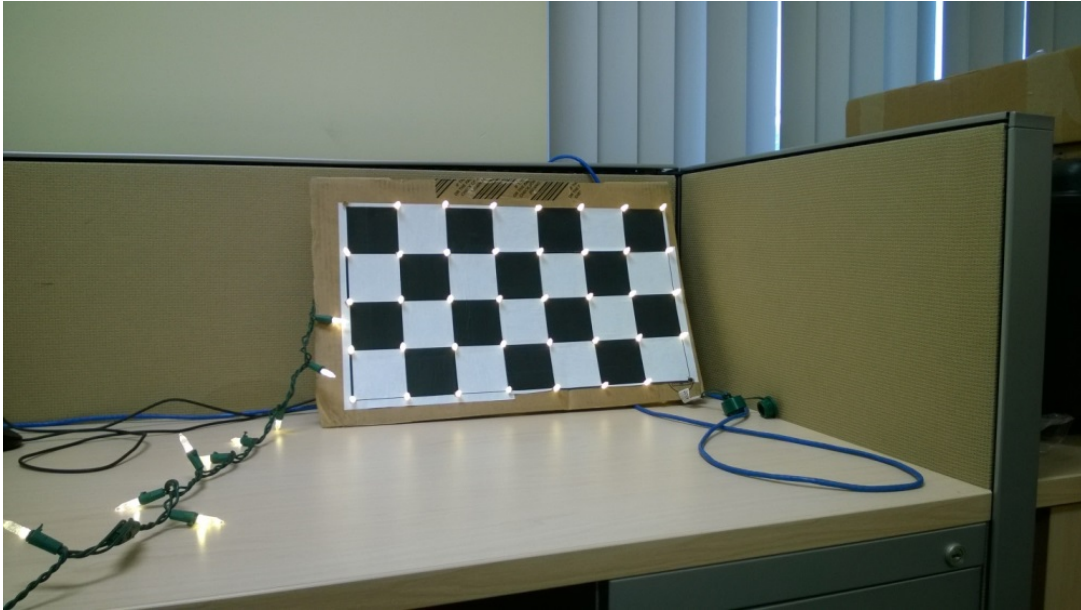
Figure 8 The LED Calibration Pattern

Figure 9 The FLIR Infrared Camera

The process of camera calibration includes estimating the infrared camera poses by finding correspondence between multiple images taken from different angles. A Matlab program that can

automatically find the correspondence of the LED lights in different images is used to estimate the poses of infrared cameras (Figures 9 to 11).

The red crosses should be close to the image corners
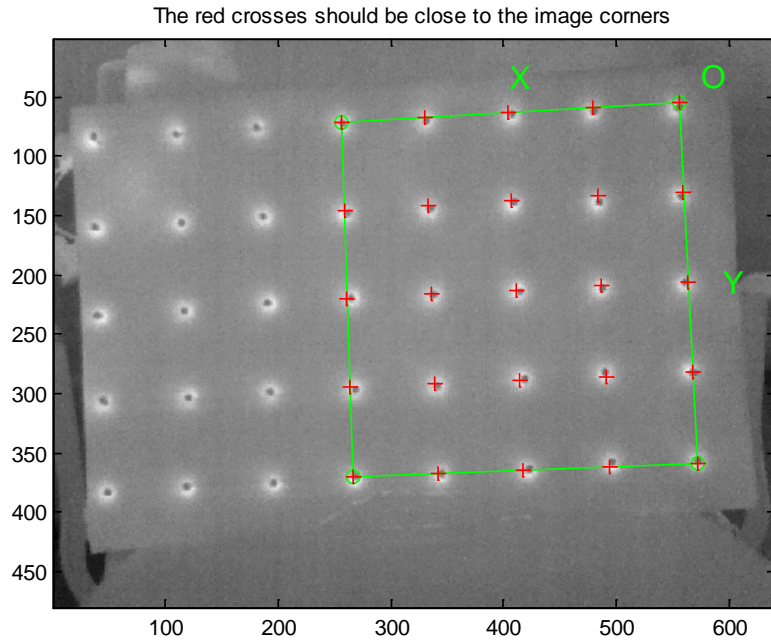
Figure 10 Heat Signature Detection

Extrinsic parameters (camera-centered)
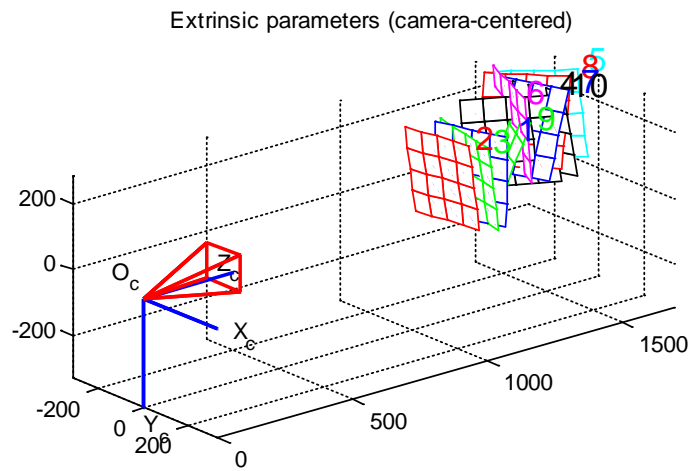
Figure 11 Extrinsic Parameter Estimation (Camera-Centered)
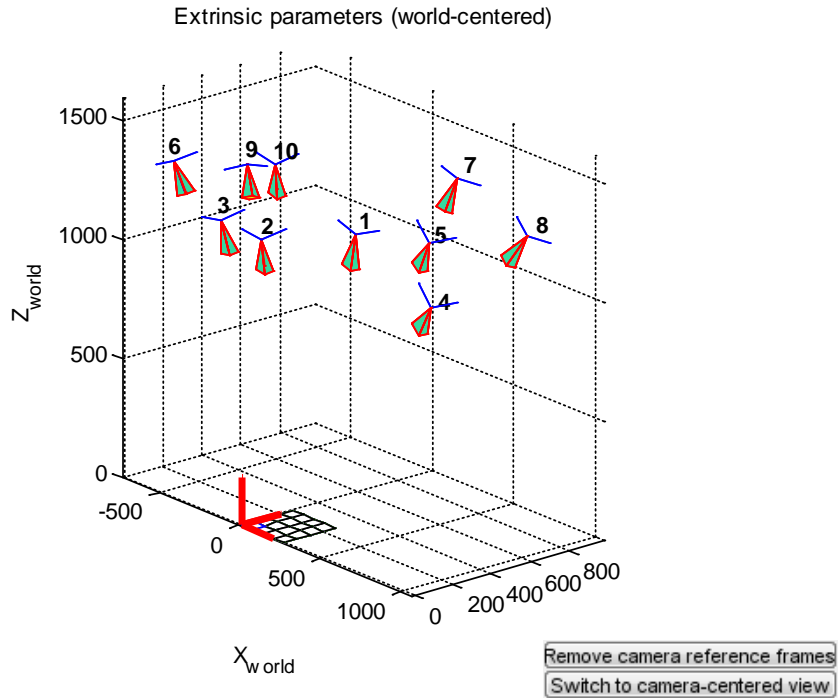
Figure 12 Extrinsic Parameter Estimation (World-Centered)

The calibration results are shown as follows (with uncertainties):

Focal Length:　　　fc = [1461.52892　1451.34718] ± [153.39188　139.22580]

Principal point:　　cc = [485.41274　282.93461] ± [137.32049　84.81277]

Skew:　　　　alpha_c = [0.00000] ± [0.00000]　 => angle of pixel axes = 90.00000 ± 0.00000 degrees

Distortion:　　　kc = [0.13026　1.33587　0.03097　0.05555　0.00000] ± [0.57429　5.07524 0.03402　0.05597　0.00000]

Pixel error:　　　err = [1.33475　1.28942]

KK=

　1461.52892　　　0.00000　485.41274

　　0.00000　1451.34718　282.93461

　　0.00000　　　0.00000　　1.00000

Calibration between Image and Point Cloud: The calibration between infrared thermography and lidar scans was done through a projection estimation. Denote a point as $C = [X, Y, Z, 1]^T$, and a pixel as $c = [u, v, 1]^T$. The projection from a 3D point on to a 2D pixel could be expressed as:

22

$$c = A[R|t]C \quad\quad (1)$$

Where

$$A = \begin{bmatrix} \alpha & \gamma & u_0 \\ 0 & \beta & v_0 \\ 0 & 0 & 1 \end{bmatrix}$$

$$R = R_x(roll) \cdot R_y(pitch) \cdot R_z(yaw)$$

$$= \begin{bmatrix} 1 & 0 & 0 \\ 0 & \cos(roll) & \sin(roll) \\ 0 & -\sin(roll) & \cos(roll) \end{bmatrix} \begin{bmatrix} \cos(pitch) & 0 & -\sin(pitch) \\ 0 & 1 & 0 \\ \sin(pitch) & 0 & \cos(pitch) \end{bmatrix} \begin{bmatrix} \cos(yaw) & \sin(yaw) & 0 \\ -\sin(yaw) & \cos(yaw) & 0 \\ 0 & 0 & 1 \end{bmatrix}$$

$$t = [x, y, z]^T$$

Denote the projection matrix as $P = A[R|t]$, for each pair of points $C_i = [X_i, Y_i, Z_i, 1]^T$, and $c_i = [u_i, v_i, 1]^T$, equation (1) could be rewritten as:

$$\underbrace{\begin{bmatrix} X_i & Y_i & Z_i & 1 & 0 & 0 & 0 & 0 & u_iX_i & u_iY_i & u_iZ_i & u_i \\ 0 & 0 & 0 & 0 & X_i & Y_i & Z_i & 1 & v_iX_i & v_iY_i & v_iZ_i & v_i \end{bmatrix}}_{G_i} \begin{bmatrix} P_{11} \\ P_{12} \\ P_{13} \\ P_{14} \\ P_{21} \\ P_{22} \\ P_{23} \\ P_{24} \\ P_{31} \\ P_{32} \\ P_{33} \\ P_{34} \end{bmatrix} = \begin{bmatrix} 0 \\ 0 \end{bmatrix} \quad\quad (2)$$

The projection matrix $p = [P_{11}, P_{12}, ..., P_{43}]^T$ then could be solved by

$$\min_P \|Gp\|^2 \ s.t. \|p\| = 1 \quad\quad (3)$$

After the projection matrix P has been estimated, the intrinsic parameters and extrinsic parameters could be retrieved as follow:

Denote $P = A[R|t] = [B \ b]$, therefore $B = AR, b = At$. Since rotation matrix is orthogonal, we have

$$K = BB^T = AR \cdot (AR)^T = ARR^TA^T = AA^T = \begin{bmatrix} \alpha^2 + \beta^2 + u_0^2 & u_0v_0 + \beta\gamma & u_0 \\ u_0v_0 + \beta\gamma & \beta^2 + v_0^2 & v_0 \\ u_0 & v_0 & 1 \end{bmatrix} =$$

$$\begin{bmatrix} k_u & k_c & u_0 \\ k_c & k_v & v_0 \\ u_0 & v_0 & 1 \end{bmatrix} (4)$$

Therefore, the intrinsic parameters are computed as:

23

$$u_0 = K_{13}, v_0 = K_{23}, \beta = \sqrt{k_v - v_0^2}, \gamma = \frac{k_c - u_0 v_0}{\beta}, \alpha = \sqrt{k_u - u_0^2 - \gamma^2}$$

And the rotation matrix and translation vector could be computed as:

$$\boldsymbol{R} = \boldsymbol{A}^{-1}\boldsymbol{B}, \boldsymbol{t} = \boldsymbol{A}^{-1}\boldsymbol{b} \qquad (5)$$

Since one characteristic of rotation matrix is $\det(\boldsymbol{R}) = 1$. However, a rotation matrix estimated by equation (5) does not necessarily satisfy $\det(\boldsymbol{R}) = 1$, which will give incorrect rotation angles. To deal with this, a nonlinear optimization procedure is used to estimate the best calibration parameters. Denote a function $\tilde{c}_i = f(C_i, roll, pitch, yaw, x, y, z, \alpha, \beta, \gamma, u_0, v_0)$ that projects a 3D point onto a 2D image plane. The objective function could be defined as

$$\|c_i - \tilde{c}_i\| = \|c_i - f(C_i, roll, pitch, yaw, x, y, z, \alpha, \beta, \gamma, u_0, v_0)\| \qquad (6)$$

The best parameters are then estimated by solving the non-linear optimization problem defined as

$$\left[\widetilde{roll}, \widetilde{pitch}, \widetilde{yaw}, \tilde{x}, \tilde{y}, \tilde{z}, \tilde{\alpha}, \tilde{\beta}, \tilde{\gamma}, \widetilde{u_0}, \widetilde{v_0}\right] = \min_P \Sigma_i \|c_i -$$

$$f(C_i, roll, pitch, yaw, x, y, z, \alpha, \beta, \gamma, u_0, v_0)\| \qquad (7)$$

As shown in Figure 12, 11 pairs of corresponding points are manually extracted, these points are used to estimate the calibration parameters. The initial calibration parameters are estimated using equation (3), and the re-projection error is shown in Figure 13 (a). It is observed that the initial calibration parameters are not accurate enough to obtain a small re-projection error. Figure 2 (b) shows the re-projection error using the calibration parameters estimated using a non-linear optimization procedure described in equation (7). Compared with Figure 2 (a), it is easily observed that the re-projection error is significantly reduced. Figure 14 shows the result of colored point cloud using this approach.
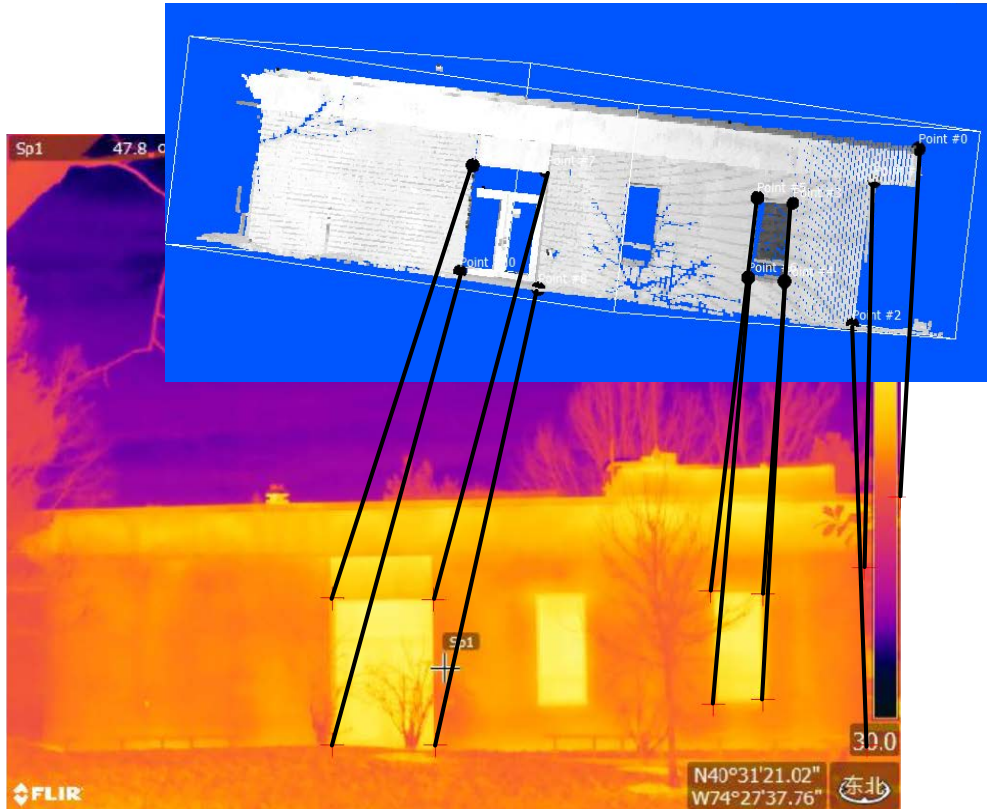
Figure 13 Estimation of Projection between Lidar and Infrared Thermography

(a)

(b)
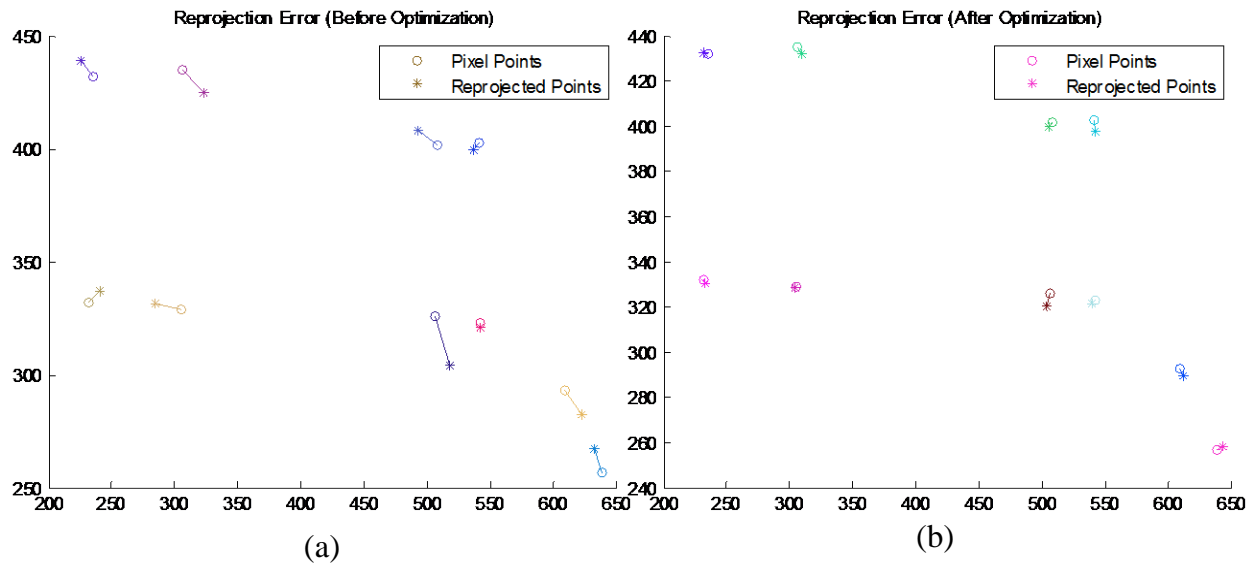
Figure 14 Summary of Re-projection Error
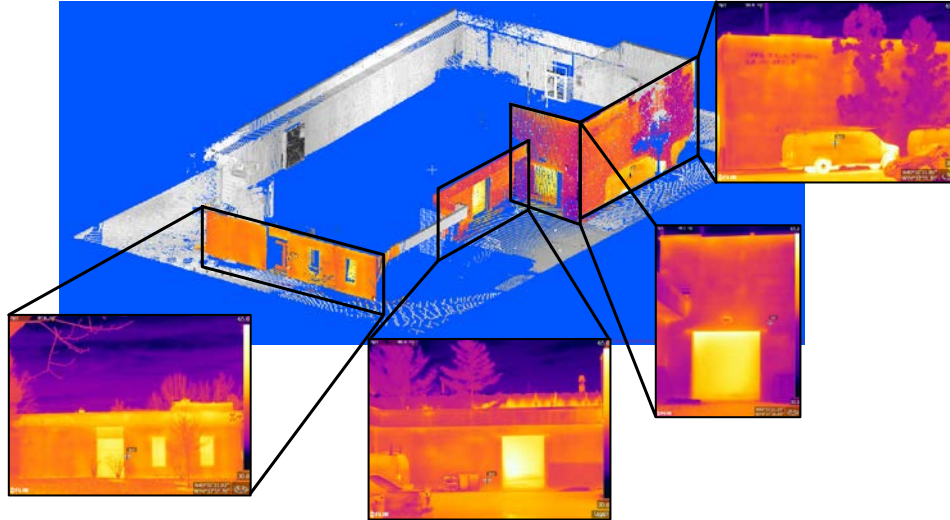
Figure 15 Colorized Point Clouds with Infrared Thermography Data

We have also developed dedicated software programs to accurately geo-reference all the lidar and infrared scan data into a common coordinate system. The following is a user interface to accomplish the task of geo-referencing lidar data. Figure 17 shows a scanned community with the developed system.
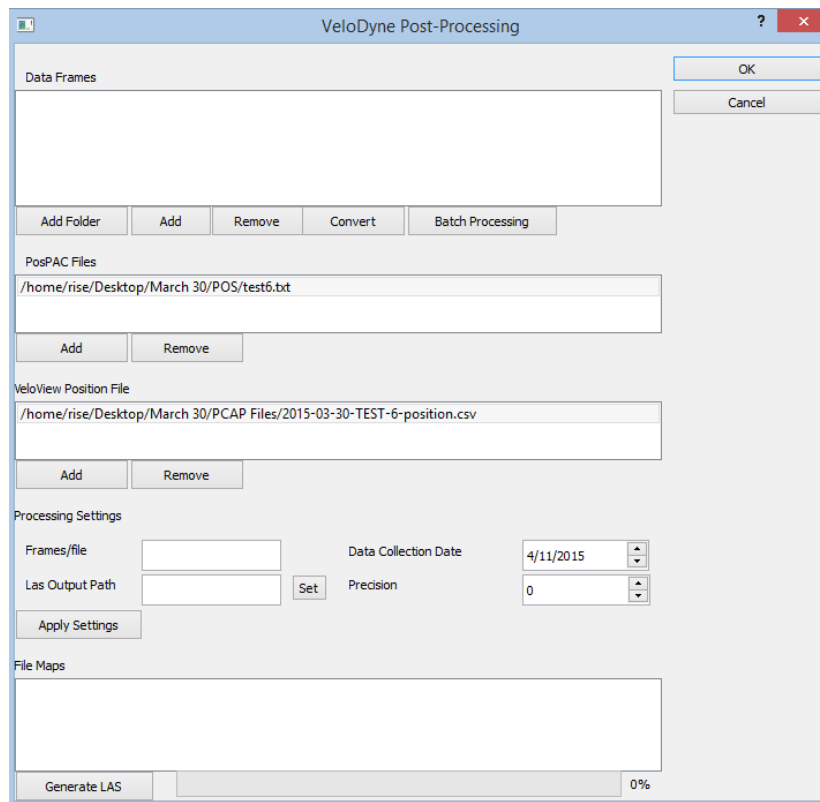
Figure 16 The LiDAR Data Georeferencing Module

26
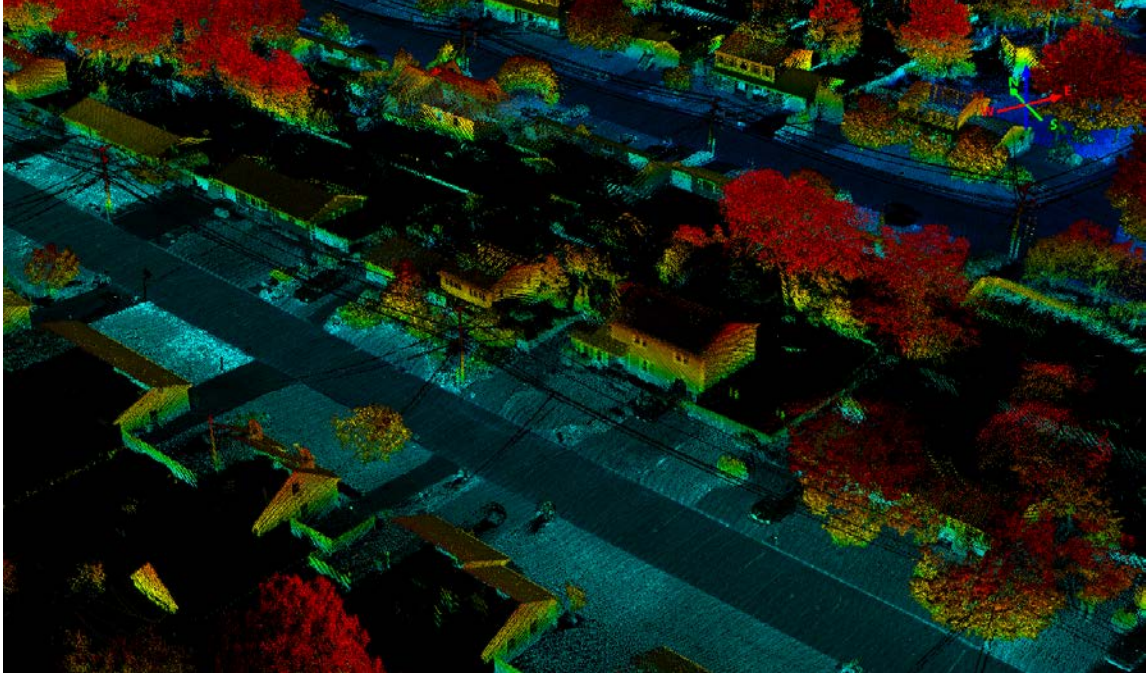
Figure 17 A Scanned Community by the Developed System

The software is now capable of processing infrared photos and geotagging the photos. The geotagged photos can be shown in Google Earth for reviewing (Figure 18).
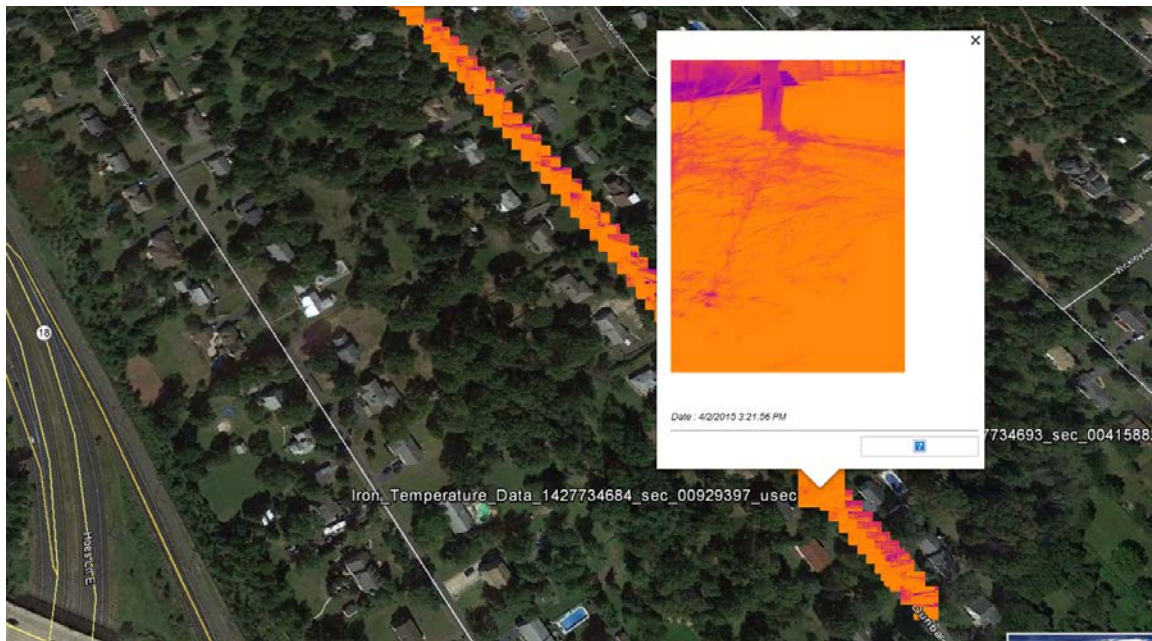
Figure 18 Geotagged Infrared Photos

The choice of infrared thermography as the gas leak detection sensor is based on careful review and evaluation of infrared thermography technology. We have conducted a field test at

NYSEG's testing facility to test the capability of infrared thermography based gas leak detection technology (Figure 19). Our results have shown this technology allows detection and visualization of leaking gas at larger distance (Figure 20-23), perhaps the most attracting capability is to detect underground gas leaks (Figure 24).

Figure 19 NYSEG Testing Facility
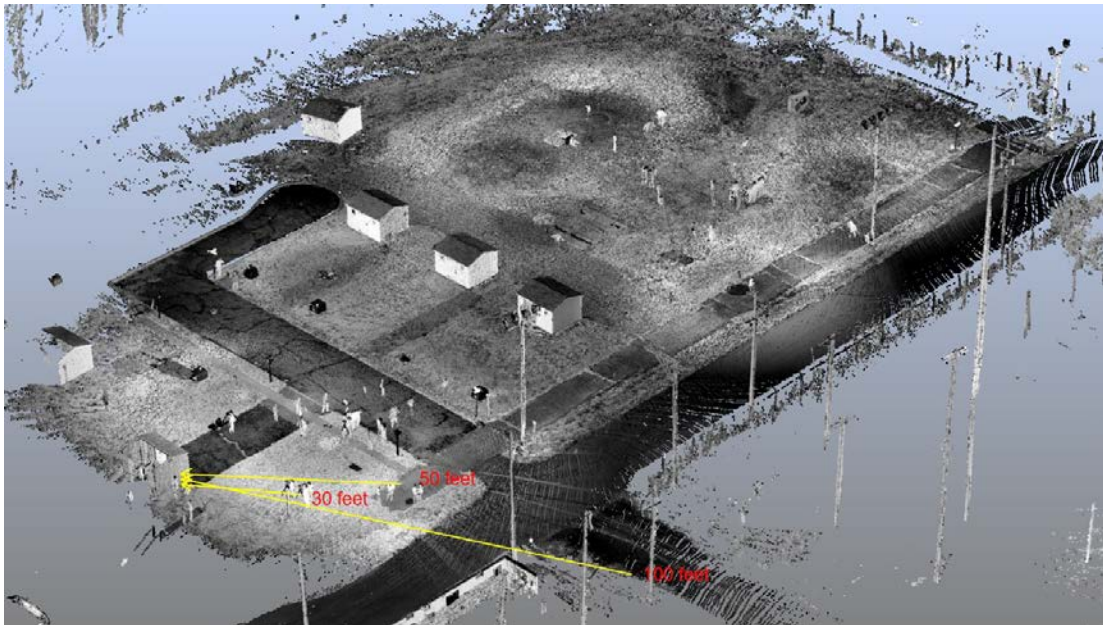
Figure 20 Detecting Gas Leaks at Different Distances
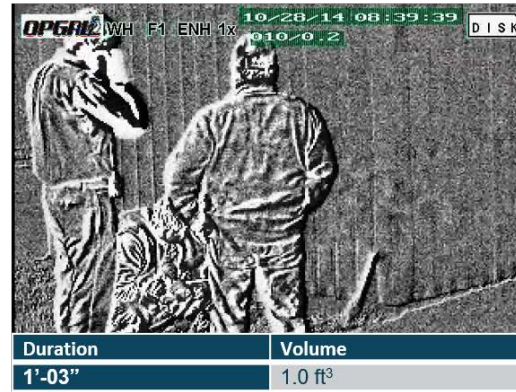
Figure 21 Successful Detection of Gas Leaks at 30 feet Distance
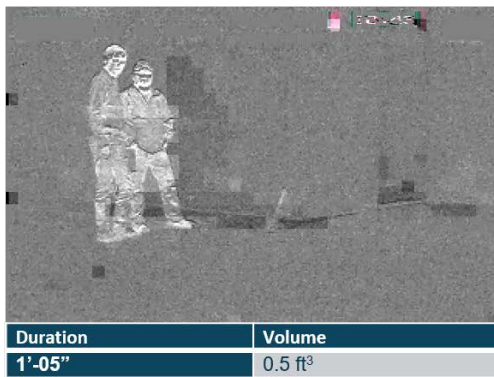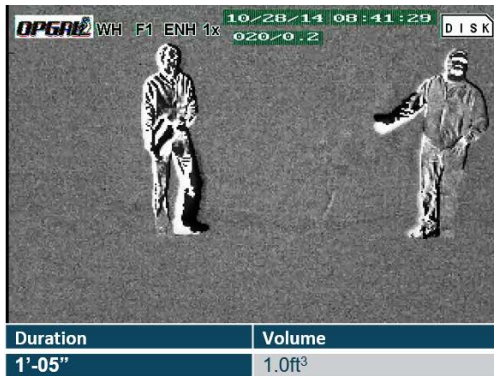
Figure 22 Successful Detection of Gas Leaks at 50 feet Distance

Duration	Volume
1'-05"	1.0 ft^3

Duration	Volume
1'-02"	0.5 ft^3

Figure 23 Successful Detection of Gas Leaks at 100 feet Distance

44

Figure 24 Successful Detection of Underground Gas Leaks at 50 feet Distance

CHAPTER 3. THREAT INDICATOR DETECTION

Natural gas pipeline failures during a natural disaster are often related to changes in the built environment (structures, terrain, etc.,) adjacent to pipelines. Table 1 lists common pipeline threats and related indicators caused by natural disasters. Our ability to quantify these indicators (parameters) will have significant impacts on our capability to identify high risk pipe segments. A framework for using these indicators to assess the risk of natural gas pipeline networks is shown in Figure 25. The rationales of this framework include the following: 1) for aboveground pipelines and gas meters, the assessment is conducted based on the assessment of building changes and damage; and 2) for buried pipelines, the main threats indicators are soil movement and flooding height. There are four types of building conditions considered in this framework. They are "no damage", "minor damage", "major damage", and "total damage". The first two conditions will lead to a decision to inspect the aboveground pipeline segments, while the latter two will lead to a decision to replace them. Regarding underground pipeline facilities, the framework requires information including soil settlement, vertical soil movement, horizontal soil movement, and flooding heights to estimate pipeline strain in order to draw conclusions about the probability of failure. A Finite Element Analysis (FEA) is then used to estimate the potential pipeline strains once soil movement and flooding height are quantified. Calculated pipeline strains were further imported into a pipeline risk analysis program to estimate probability of failure. The details about this risk assessment framework are explained in Task 4's accomplishment. It can be seen that the success of this framework depends on our capability of quantifying changes in building conditions and soil movement as well as identifying water levels resulting from flood. This task focuses on developing a geospatial data analytics workflow to quantify the essential threat indicators including building displacement, flooding height, and soil movement.

Table 1 Pipeline threat and related indicators

Threat	Cause	Phenomenon	Indicator
Water Infiltration	Pressure Head	Water Level Resulting from Flood	Water Elevation Above Ground Surface
Underground Pipe Break	Strain	Soil Deformation Resulting From Flood, Landslide, Hurricane, and Earthquake	Soil Displacement

Above Ground Pipe Break	Strain	External Force from Flood, Landslide, Hurricane, Earthquake, Tornado	Asset Displacement
Exposed Pipe	Soil Erosion	Soil Erosion Resulting From Flood, Landslide, Hurricane, Earthquake	Soil Displacement
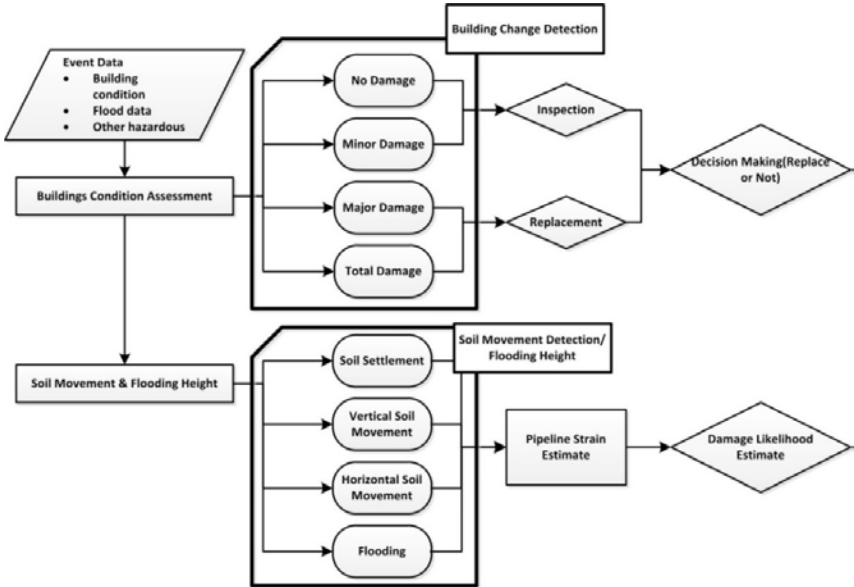
Figure 25 Proposed Post-disaster Pipeline Risk Assessment Framework

A novel multi-resolution building and terrain change detection framework is proposed for computing essential threat indictors that are required in post-disaster pipeline risk assessment. In this framework, airborne and mobile lidar data collected before a disaster are used as reference data, and lidar data captured after a disaster are treated as target data. Changes are computed by comparing target data against reference data. A pipeline distribution network is treated as two separate systems in this framework: 1) aboveground pipeline segments and gas meters; and 2) buried pipeline segments. For assessing conditions of buried pipeline segments, terrain changes are computed to estimate possible pipeline displacements. Such displacements can be caused by soil movement in both vertical and horizontal directions and debris loads. The proposed framework also focuses on quantifying building displacements and their associated impacts on aboveground pipeline segments and gas meters. The entire change analysis workflow is shown in Figure 26. It can be noted that the workflow has essentially two main stages where change

detections are conducted at different resolutions. A detail description of each stage is presented in the following paragraphs.

Low-Resolution Stage

In this stage, airborne lidar data are used as the spatial data source for change detection. The change detection is conducted using only ground and building classes in the pre- and post-event lidar data. Therefore, the work flow starts with point classification. In this paper, a progressive morphological filter algorithm [34] is used to classify lidar data into ground points and non-ground points. After this step, the non-ground points could still contain multiple classes of objects such as building, vehicle, pedestrian and vegetation. At this point, change detection is conducted on both ground and non-ground points. Multiple algorithms [35, 36, 37] are available for measuring changes between point cloud data. In this research, a point-to-point distance D_i between two point sets $\{\mathbf{P}, \mathbf{Q}\}$ is used as the change detection method, and it can be expressed as the following:

$$D_i = \min_j \|\mathbf{p}_i - \mathbf{q}_j\| \qquad (1)$$

where $\mathbf{p}_i \in \mathbf{P}$ and $\mathbf{q}_j \in \mathbf{Q}$.

In general, change detection results can be visualized using heat map based visualization where large changes are colored with hot colors. This makes it straightforward for identifying areas with large changes. In this paper, dune erosion, scour, and debris from eroded dunes and displaced buildings are major changes that can be detected from such change analysis. Areas with severe building displacement and soil movement are high risk regions, which require further change analysis at a higher spatial resolution.
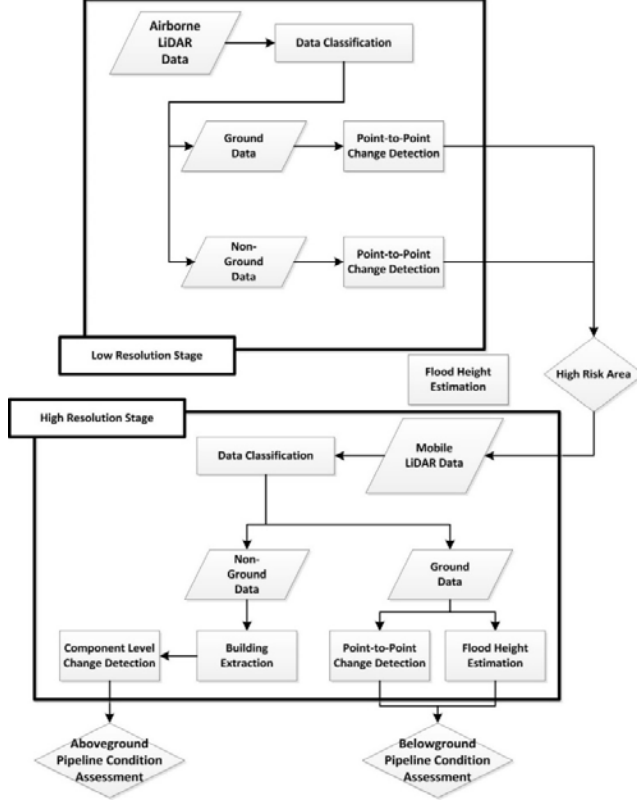
Figure 26 Proposed Framework of Pipeline Post-Disaster Condition Assessment

High-resolution Stage: In this stage, mobile lidar data are added to spatial data source for high resolution analysis. The same filter employed in the low-resolution stage is employed to classify mobile lidar data into ground and non-ground classes. In this stage, a pipeline network is also separated into buried and aboveground parts, and each of those requires a different change analysis workflow.

1. Buried Pipeline Assessment

For ground points, the point-to-point distance D_i (Equation (1)) is computed at first to obtain the magnitude of change. Since directions of soil movement are related to different types of pipeline failure modes, this requires change to be calculated along different directions. Therefore, terrain changes at this step are computed along the x, y, and z axes. For each pair of points $\{\mathbf{p}_i \in \mathbf{P}, \mathbf{q}_j \in \mathbf{Q}\}$, the change along the direction d is assigned positive if the component at d of $\mathbf{p}_i$ is to the positive side of the component at d of $\mathbf{q}_j$, and vice versa. This could be expressed as

$$D_i^d = \begin{cases} \min_j\{p_i^d - q_j^d\} \\ -\min_j\{p_i^d - q_j^d\} \end{cases} \tag{2}$$

34

where p_i^d is the component of point $\mathbf{p}_i$ at the d direction, and $d = x, y, z$.

In addition, flooding heights are measured from high water marks in georeferenced photos collected along with mobile lidar data. Since such street-view imagery were registered with mobile lidar data, this makes is possible to recover 3D geometric information of features (high water marks) in the images by treating the images and lidar data as stereo pairs. The recovered information about high water marks can be used to estimate water pressure placed on the pipeline network during storm events.

2. Aboveground Pipeline and Gas Meter Assessment

To assess aboveground pipeline segments, it is important to determine building damage conditions from change analysis. This starts with building extraction from lidar data. One feature that distinguishes buildings from other non-ground objects such as vegetation and vehicles is that buildings contain multiple planar objects such as walls and roofs. Therefore, it is possible to use flatness of points as a criterion for building extraction. Another feature useful for building segmentation is the size of building objects. Although billboards and vehicles may contain planar objects, the sizes of these objects are normally smaller than that of building objects. In this study, a combination of Euclidean distance based segmentation algorithm and region growing segmentation algorithm is used to extract buildings from lidar data. The extracted buildings could be used to analyze changes in building structures at the entire building level.

To further quantify building conditions, a building component level change detection approach is also developed in this study. In this approach, building components are extracted from point cloud data using a sophisticated clustering method that is built on top of the RANSAC algorithm [38], a density based clustering method, and a cluster matching algorithm. The description of these methods is beyond the scope of this paper. Kashani and Grattinger (2015) provides a detailed analysis on point cloud features that can be used in clustering methods to extract planar objects such as roof covering [39]. Kashani et al. (2015) also discussed the use of intensity data for wind damage detection [40]. In the nutshell, this method segments building into planar objects, classifies these objects into different building components, and matches these building components in pre- and post-event data. Therefore, it enables comparison of building conditions at individual component level, leading to a fine classification building conditions. Such building condition data will form the foundation for assessing whether the attached gas facilities are likely damaged or not.

Software development: Based on the above principle, we have developed a damage indicator detection software package (Figure 27). The software package includes three modules for extracting damage indicator information from remotely sensed data. The following provide detail explanations for each module.
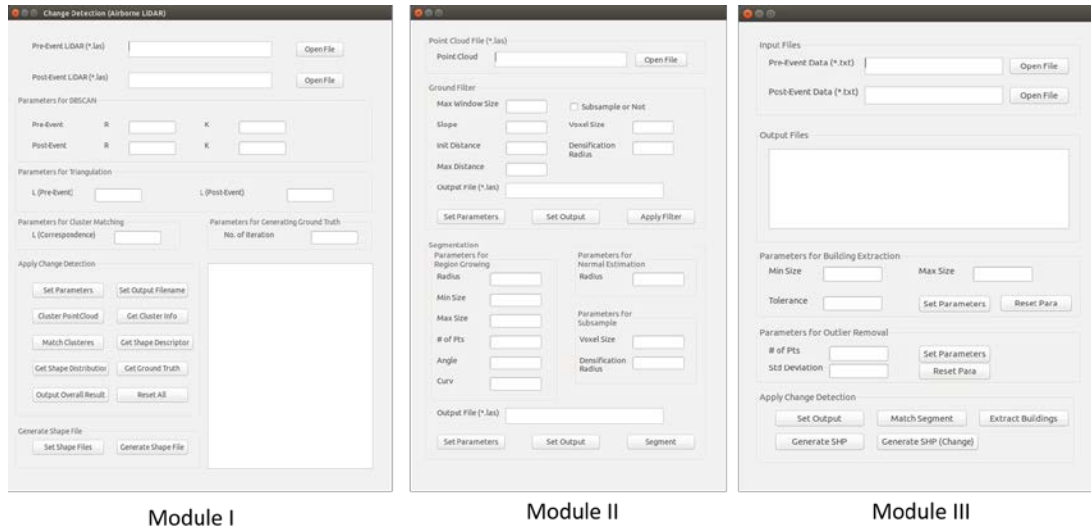
Figure 27 Threat Detection Software Modules

Module I: Airborne LiDAR Change Detection

This Module does the following tasks:

1) Clusters the Point Cloud into Buildings;

2) Detect the changes between Pre- and Post- event data sets;

3) Output the change detection information for damage analysis;

4) Generate the Shapefile of each building clusters.

Module II: Point Cloud Processing:

This Module implements the following tasks:

1) Grounding Point Filtering;

2) Surface Segmentation;

The GUI of this Module is shown as follows:

Module III: Mobile LiDAR Change Detection:

This Module does the following tasks:

1) Extract building clusters from Mobile LiDAR data;

2) Detection changes between Pre- and Post- event Mobile LiDAR data sets;

3) Generate the Shapefile of each building clusters.

The GUI of this Module is shown as follow.

Case Study: A case study is conducted to validate the proposed methodology. Hurricane Sandy related spatial data sources including pre-t and post-event airborne and mobile lidar data are used in this validation. Due to the lack of pre-event mobile lidar data, mobile lidar data collected after community rebuilding are employed as the pre-event data set. The difference between real pre-event (before Hurricane Sandy) and simulated pre-event (after recovery) does not affect the validation of proposed methodology. This is because the scope of this research is not on measuring the damage caused by Hurricane Sandy, but on the capability of change detection.

Change Detection at the Low Resolution Stage

The results of change detection using pre-event and post-event airborne LiDAR data are shown in Figure 28. The point clouds were classified into two categories: 1) ground; and 2) buildings. The changes (either negative or positive) in each category are displayed in four different colors. The yellow and cyan represent the sand debris and eroded dunes respectively, and the points colored in red shows the damaged buildings. The sand debris and eroded dunes are indicators of terrain changes and their volumes can be quantified and overlaid on a pipeline network to estimate the amount of pipe strains due to these changes. The areas with damaged buildings show the need of repairing or replacing aboveground gas risers and meters.

(a) Sand Dunes & Debris   (b) Detection of Debris, Dunes and Damaged Buildings
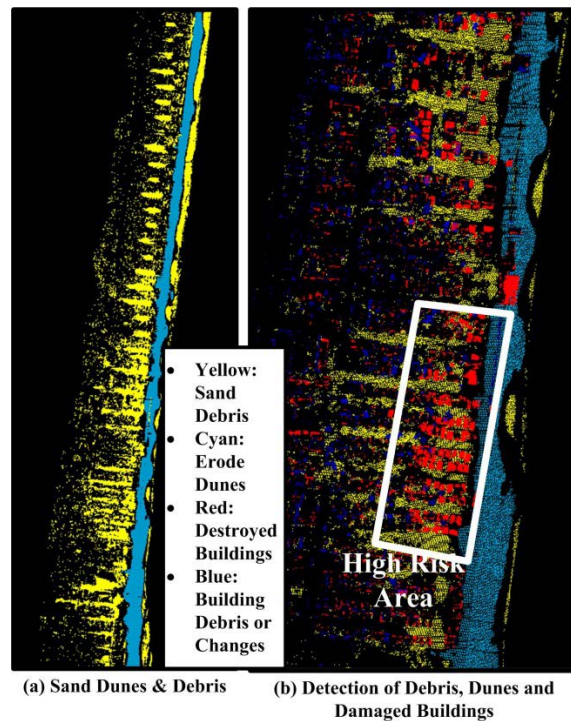
Figure 28 Low-Resolution Change Detection Results

37

Change Detection at the High Resolution Stage

In this stage, the buildings are first extracted from the mobile lidar data with the approach described in the previous section. The extraction results are shown in Figure 29. Figure 29 (a) and (b) show the original mobile lidar point cloud data before classification (the color coding represents elevations. The data are then classified into ground and non-ground points as shown in Figure 29 (c) and (d), where blue points represent the non-ground objects and red points represent the ground. Figure 29 (e) and (f) shows the results after applying building extraction and building component segmentation. It can be seen that most of the points belonging to buildings are extracted and the vegetation, vehicles and other non-building points are mostly removed. The point clouds with different colors in Figure 29 (e) and (f) represent different building components.

A point-to-point based change detection is then conducted on the high-resolution mobile lidar data to evaluate the changes in both terrain and building conditions along the x, y, and z directions. The results are shown in Figure 30. There are a number of observations that can be drawn from this Figure 30(a): (1) the terrain (ground) changes along the x and y directions are very small, indicating no or small change at the horizontal directions; (2) the terrain change along the z direction has a wider distribution compared to that of the other two directions; (3) almost 62% of the points from the post-event data are lower than the points from the pre-event data; and (4) there is an increased load to the buried pipelines in the areas where the change detection results are shown as green and cyan color. The uneven distribution of vertical soil loads due to terrain change can potentially cause bending and vertical displacements to the buried pipelines, which increases the potential risk of pipeline failures. For building change detection, a large change value implies the building is destroyed, and a small change value implies the building is partially damaged. The color mapped changes in building conditions are shown in Figure 30(b) and (c). Figure 30 (c) is a zoom-in view of the changes for a few buildings. These plots clearly indicate changes along the x, y, and z directions.
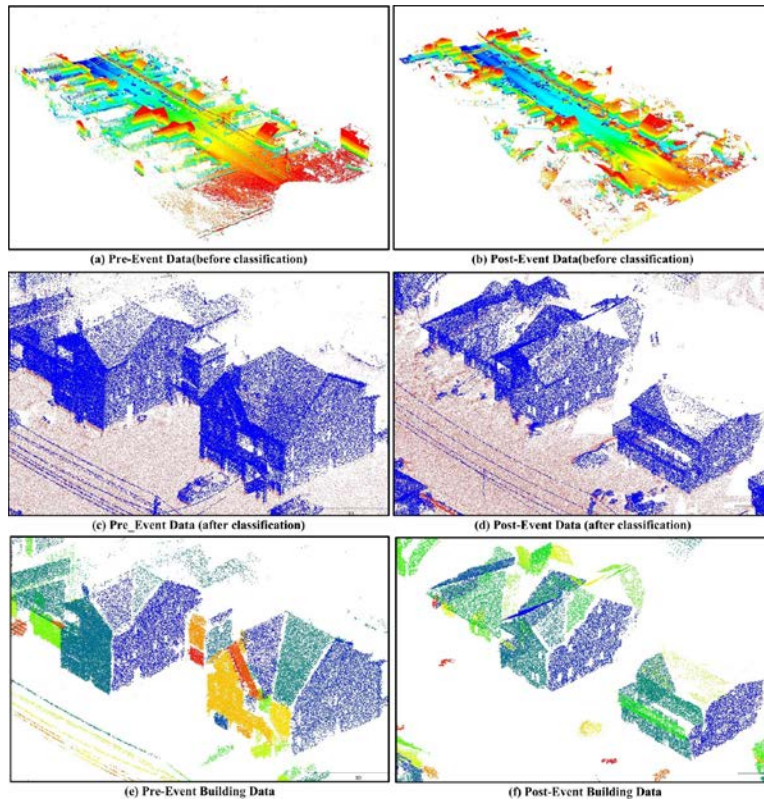
Figure 29 Building Extraction from Mobile Lidar Data
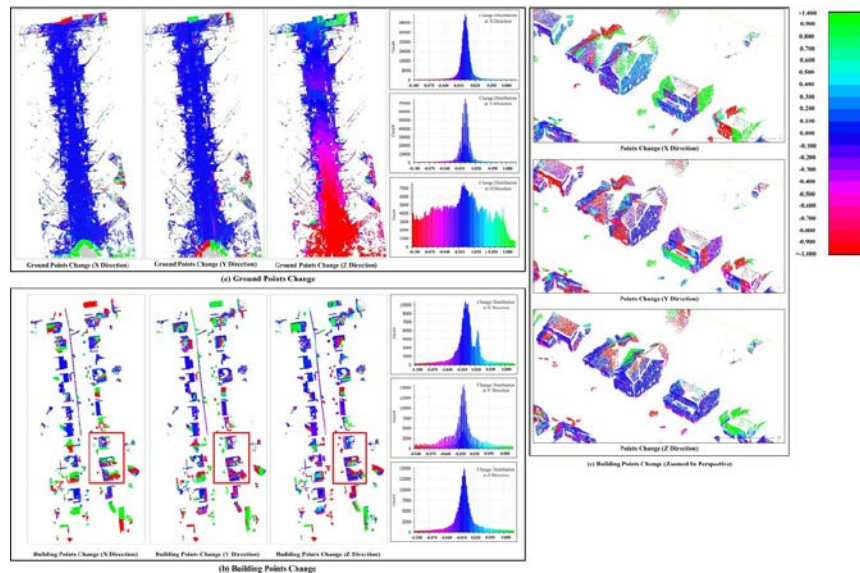
Figure 30 Change Detection Results at the High Resolution Stage

The change analysis at this stage can also be conducted at the building component level. The results of such analysis are shown in Figure 31, where the planes colored in blue indicate no observable changes along the direction perpendicular to their surfaces and the planes colored in

red indicate significant changes (>= 5 meters). The changes in between these levels are colored from cyan to orange representing gradually deteriorating conditions. Based on this scheme, the following observations can be made: (1) the component level change detection (Figure 31(c)) suggests there is no damage to the roof structure while a 0.10-meter change has been detected on the front facet indicating a potential damage to the wall panel; (2) a 0.5-meter change has been detected on the side wall noted in the red box in Figure 31(c), indicating potential damages to gas risers or meters connected to this wall; and (3) large changes to the components of Building 1 have been detected indicating very severe change or a potentially total damage (Figure 31d and e). Since we used mobile lidar data after the rebuilding to simulate the pre-event mobile lidar data, this may not actually be the case. Further investigation of this building indicates that this building is totally modified after the disaster. This shows the proposed approach is capable of detecting these radical changes.
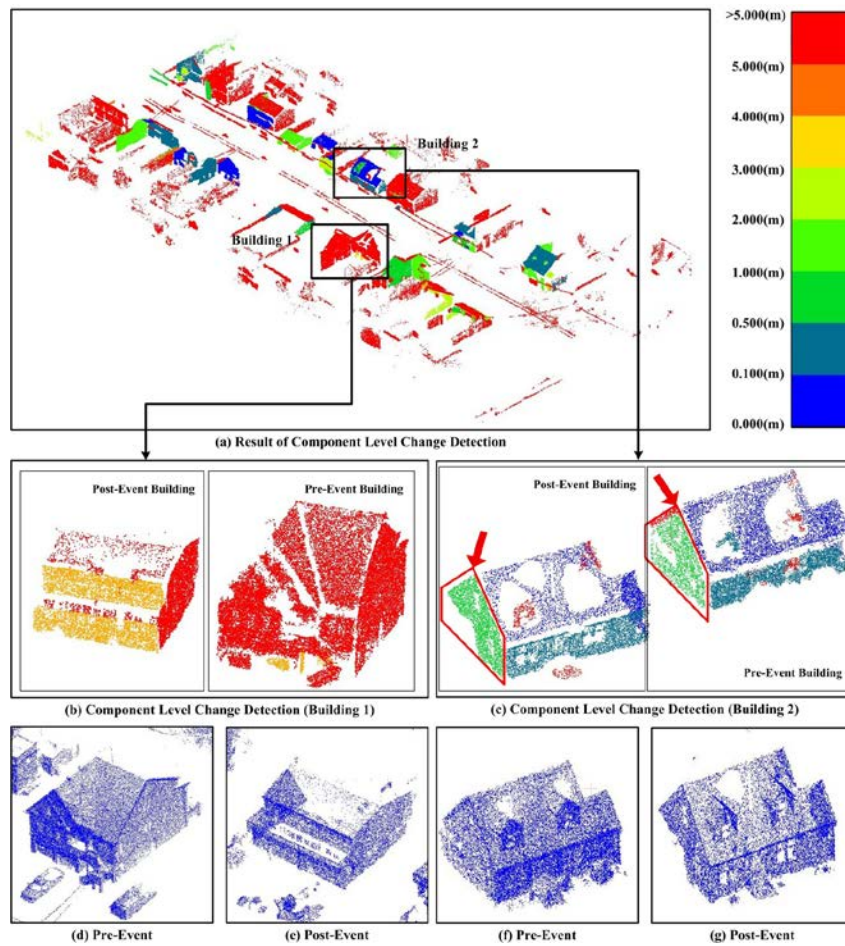
Figure 31 Change Detection Results at the Building Component Level

Storm surge generated by tropical storms is a severe threat to the integrity of natural gas pipelines. During a hurricane event, it is essential to collect data on storm surge height as it helps determine the water pressure head on the buried pipelines. With the high resolution mobile lidar data, this information can be directly measured from mobile lidar imagery. Figure 32 shows how such information can be obtained.
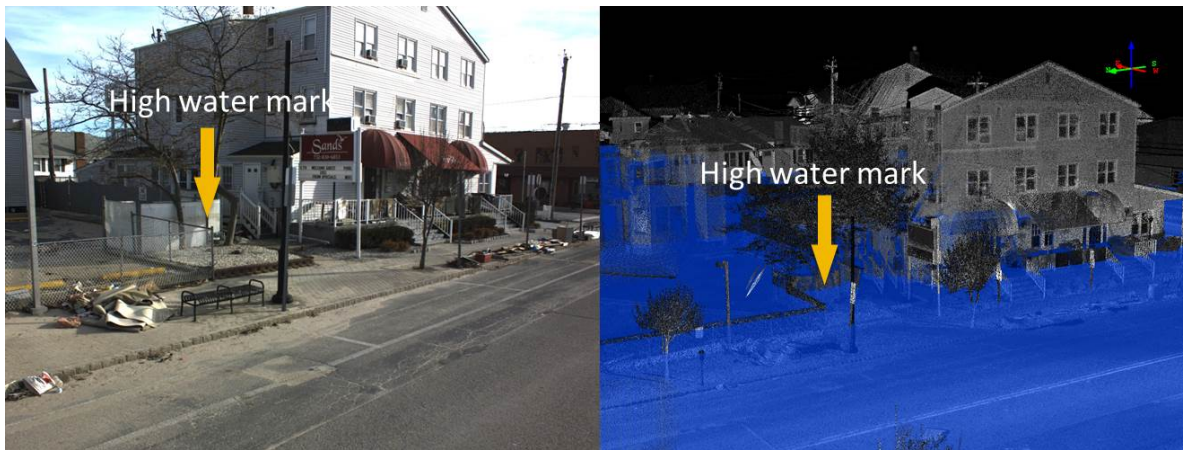
Figure 32 Measuring Storm Surge Height from Mobile Lidar Imagery

Summary of Threat Indicators

The change analysis results from both low-resolution and high-resolution data can be further interpolated and overlaid on impacted areas where pipeline locations are known. These change analysis results become critical threat indicators (Figure 33) that will be used to compute pipeline strain and pressure head – both will pose threat to pipeline integrity.
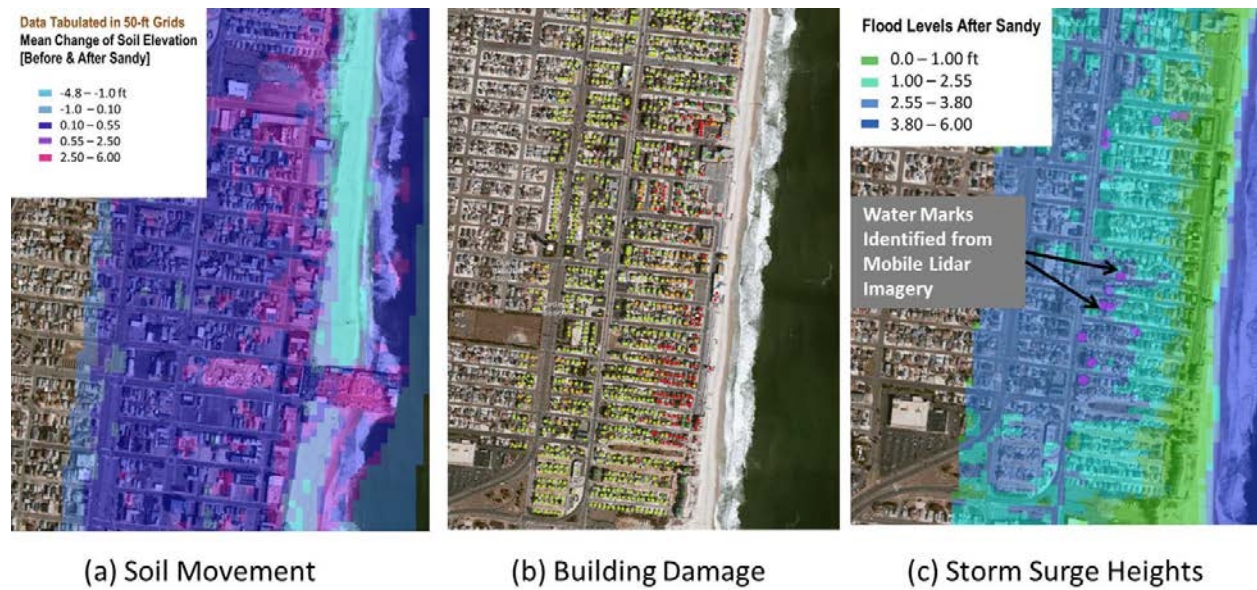
Figure 33 Computed Pipeline Threat Indicators

Integration of UAV-borne Data Sets

Two airborne data sets are used for evaluating the quality of 3D dense reconstruction from photos. The first data set was captured from a helicopter platform to simulate images taken from typical UAV platforms in the summer of 2015. The area we studied is a location with a high concentration of infrastructures. Many types of critical infrastructure systems are collocated in this location (Figure 34). Much of this area was successfully reconstructed with the captured images (Figure 35).

Figure 34 3D Dense Reconstruction Site 1
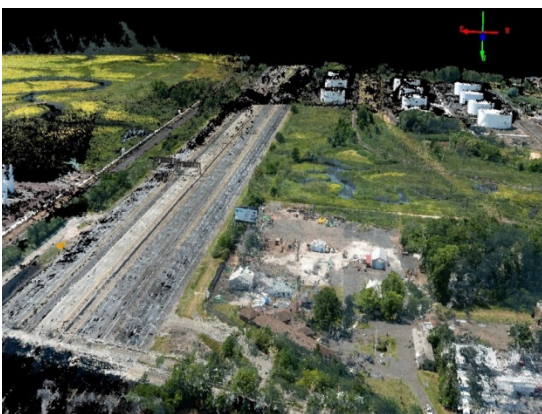
Figure 35 3D Reconstructed Area

The second dataset was captured using a large fixed wing UAV system in June 2015. The data was collected during operations at the Cape May Airport (KWWD) June 16-18 2015 using a rapid response payload InstiMaps. This first generation payload relies on a low cost GPS receiver system without any INS to provide geolocation for each image when captured. The system enables in flight download and processing of imagery for rapid dissemination. The system is based upon a low resolution 12 Mega Pixel mechanical shutter image sensor. The purpose of this payload is to provide rapid response data not survey grade information and data produced should be treated as such. As part of flight operations at KWWD three mission objectives were identified and are listed by order in which they were flown: (1) Map the area of KWWD; (2) Map power line corridor adjacent to KWWD; and (3) Image example pipeline segment.

A data tier system was used to indicate how far removed the data is from the raw sensor output. The data tier outline is as follows:

- Lv0 - Raw sensor data usually in proprietary formats
- Lv1 - Raw data converted to standard file formats
- Lv2 - Data from multiple sources fused into standard formats
- Lv3 - Multisource data fused and reduced to remove overlap, saved in standard formats
- Lv4 - Additional human interpretation added to the spatial data
- Lv5 - Spatial data converted into non-spatial abbreviated forms
- Lv6 - Results of spatial data modeling/analysis based on lower level data
- Lv7 - Reporting of spatial data statistics or report in summation
- Lv8 - Reporting of metadata regarding data collected or metadata statistics.

The images are taken using an onboard camera which was pointed vertically towards the ground. The sufficient overlap between images ensures a successful 3D reconstruction as shown in Figure 36.

Figure 36 3D Reconstruction from UAV imagery

UAS-borne remote sensing platforms are emerging systems for capturing necessary information during extreme events. Typical remote sensing data that can be captured by these systems are image data, lidar data, and infrared data. Image data are also used for dense 3D reconstruction using a structure from motion framework. At the end of the process, the end products are generally large quantities of point cloud data. Therefore, the integration of UAS-borne remote sensing data is essentially a point cloud data integration problem. The point cloud data reconstructed from UAV-borne imagery are typically scale-free, requiring additional reference points in order to becoming dimensional point cloud data. However, once the point clouds are scaled with control points with known distance, using these point clouds in our existing threat detection framework is a straightforward process. Figure 37 summarizes the adopted approach for integrating UAS-borne point cloud data into our current framework.
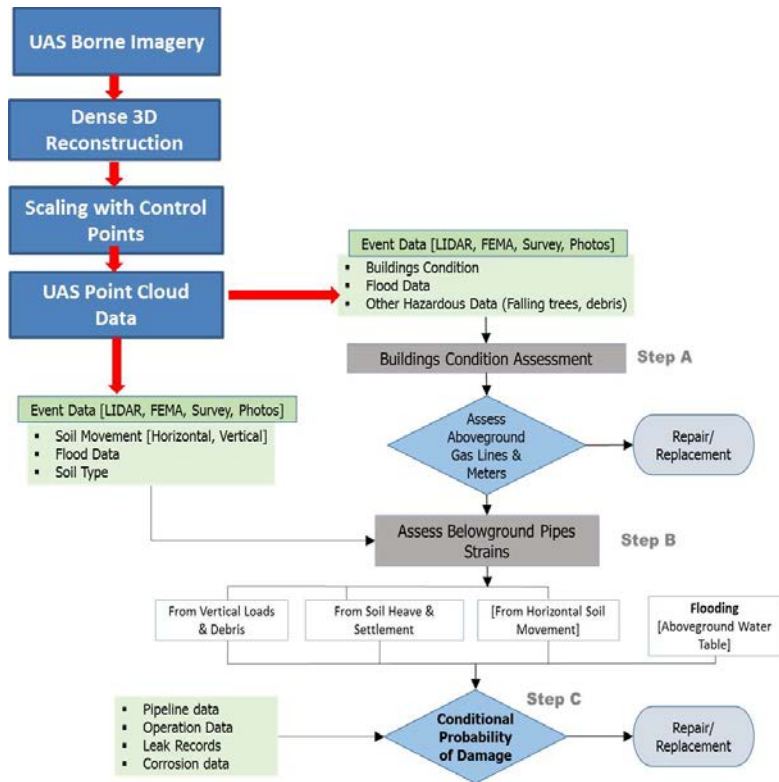
Figure 37 Integrating UAS Point Cloud Data into Risk Assessment

CHAPTER 4. PIPELINE RISK ASSESSMENT FOR DECISION SUPPORT

The focus of this task is on analyzing the effect of the detected damaging forces in Task 3 on pipeline material used in the natural gas distribution system. Differential soil displacement can result in significant deformations of buried pipes. These soil displacements are implemented in a finite element (FEA) program to estimate pipe deformations and strains for various soil properties, pipe types, and sizes. Pipeline strains are integrated with estimates of pipeline damage due to flooding to produce an overall estimate of likelihood of damage. This estimate was performed using Bayesian Network (BN) approach to produce the overall damage probability. This is accomplished by using the software program 'Agena Risk' to establish the damage likelihood. Finally, two programs are developed to incorporate the BN results to provide an estimate of the damage probability of belowground pipelines due to natural forces. One of the programs is web-based to provide users an option to use it without requiring any other specific programs. The other program is ArcGIS based since many utility operators manage their utility assets in such a program. Then it is intuitive for them to use an ArcGIS plugin program to accomplish the risk assessment tasks. The programs were used to present a case study to evaluate the natural gas pipeline system after hurricane Sandy in the coastal area at Ortley Beach in New Jersey. The example integrated the GPS pipeline system data along with the LiDAR post-disaster soil displacement and water elevations to rank the pipeline segments likelihoods of failures.

Strains in Belowground Pipes Due to Natural Forces: Gas distribution pipelines may experience high longitudinal strains in the event of soil movement resulting from slope instability, soil subsidence, seismic activity, and flooding. Currently the available pipeline design codes and standards do not provide comprehensive guidance on allowable limit deformations for strain-based loading. Several previous studies provide recommended procedures and guidelines for the assessment of pipelines subjected to large soil deformation and seismic loading conditions [18, 19, and 20]. This chapter provides an analysis of pipeline-soil interaction with respect to axial, lateral and combined soil movement on the pipe. The results of this analysis provide the limit pipe strains for quantifying the risk factors due to outside force.

Most of soil-pipeline interaction analysis represent the pipe as a structural beam with the soil represented as spring elements in the axial (longitudinal), transverse horizontal, and transverse vertical directions [21]. This simplification is derived from the concept of sub-grade reaction

originally proposed by Winkler (1867). The axial load on the pipe results mainly from the friction caused by soil shear stresses acting around the pipe circumference. As the ground displacement is progressively increased, the pipe may reach their specified compressive or tensile strain limits. Additionally, the soil may yield and continue to move past the pipe with no increased pipe deformations. Soil displacement may be taken as the upper bound of pipe displacement.

Differential soil settlement can result in significant deformation of buried pipes and above ground facilities such as gas meters. The ASME B31 code [22] indicates that large displacement stresses may be acceptable providing that excessive localized strains do not exceed their acceptable limits. Acceptable strain limits are typically based on testing and detailed analysis of the soil-pipe interactions under various ranges of the longitudinal and bending loads. The ASCE Committee on Gas and Liquid Fuel Lifelines [21] suggests the use of an elasto-plastic or a hyperbolic model for the soil resistance versus pipe movement. Several analytical models [23, 24] provide estimates of the maximum soil axial and lateral forces per unit length at the soil-pipeline interface. Pipe strains under various loading conditions were modeled using the Finite Element (FEA) program 'PIPLIN' [25]. The program is a special purpose commercially available program for stress and deformation analysis of pipelines. The program considers the effect of internal pressure, soil horizontal deformation, and settlement and it incorporates the nonlinear behavior of the pipe and soil support under large displacement effects. Tables 2 and 3 show the pipe and soil parameters used in the finite element analysis.

Table 2 Pipe Parameters for Estimating Pipe Strains

Parameters	Range of Parameters for gas distribution lines
Pipe Type	Steel Mains (grades A to X40), Plastic mains and services, and Cast iron Mains
Pipe Size	¾-6 inch, Plastic 1-4 inch, Steel 4-12 inch, Cast iron
Soil Type	Loose sand Dense sand Clay
Length of moving soil section	60, 120 feet
Vertical and horizontal soil movement	1, 2, 3, and 4 ft

Table 3 Soil Parameters Used in the Analysis

Soil	Unit Weight (lb/ft^3)	Soil Friction Angle	Soil Cohesion (lb/ft^2)
Loose Sand	120	25	0.2
Dense Sand	140	40	100
Clay	130	5	1400

Soil is modeled in the program as nonlinear 'Winkler' foundation with discrete supports. Soil movement and settlement were assumed to be applied statically. Several nonlinear aspects of pipe behavior are considered, including yield of pipe, large displacement effects, and nonlinear soil support. The strains on the pipes are highly dependent on the pipe type and its properties. The pipe types used in the analysis were steel, plastic, and cast iron pipes of various sizes. Figures 34 to 36 show the mechanical properties of these material.
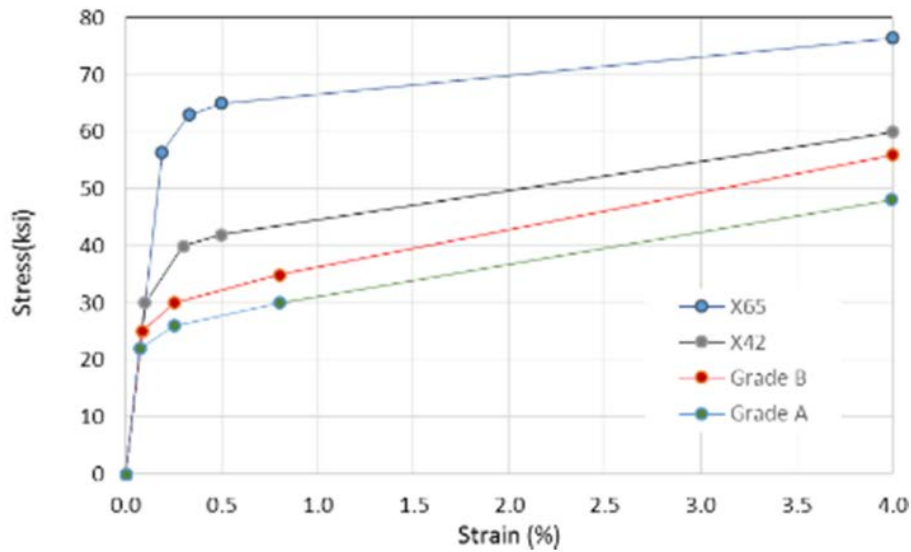
Figure 38 Stress-strain relationship of the steel pipe [26]
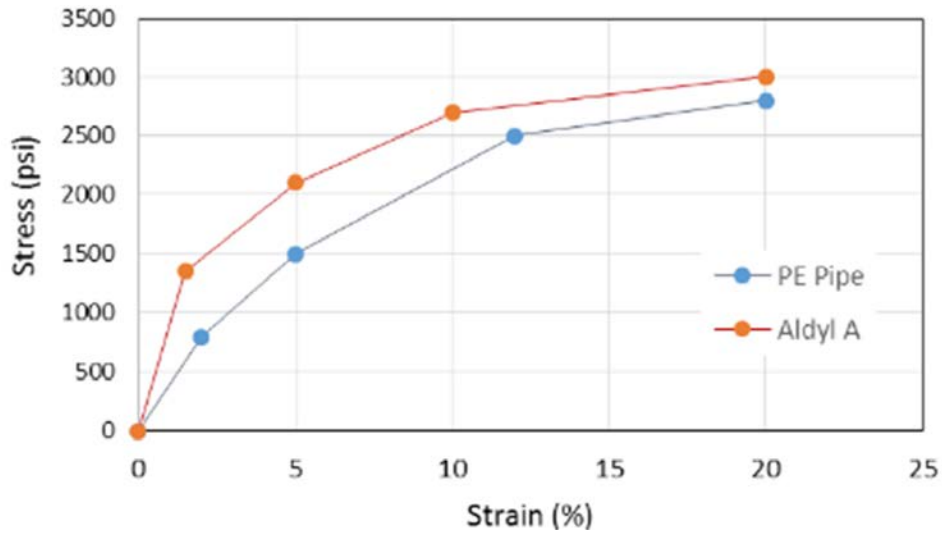
Figure 39 Stress-strain relationship of the plastic pipe [27]
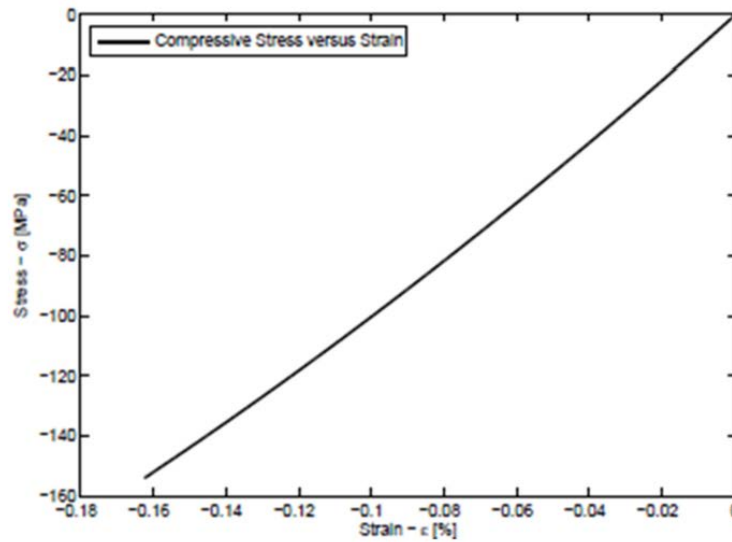
Figure 40 Stress-strain relationship of the cast iron pipe in compression [28]

Pipe Strains under Soil Movement

Pipe strains were calculated in the FEA for to the following natural forces threats:

i. Vertical soil movement and settlement,

ii. Horizontal soil movement and landslides,

iii. Flooding.

Additionally, building displacement data form the LiDAR measurements were considered in evaluating threats to aboveground facilities such as gas meters and regulators.

i. Vertical Soil Movement and Settlement

Figure 37 shows schematics of the pipe deformations under vertical soil movements. These movements can be caused by increased overburden load, depression due to loss of soil strength, or washout of an underlying soil layer. The pipe is modeled by beam type members connected by nodes in the x-y plane. In the cross section direction, the stresses and strains are calculated at a number of points (typically 30) in the cross section. Pipe yield at the monitored points is taken into account assuming the von Mises yield criterion, with nonlinear kinematic hardening. Interaction between hoop and axial stresses is taken into account. Discrete supports for pipe anchors or above ground bents are modeled as nonlinear springs. Pressure, temperature, settlement and gravity loads are assumed to be applied statically.
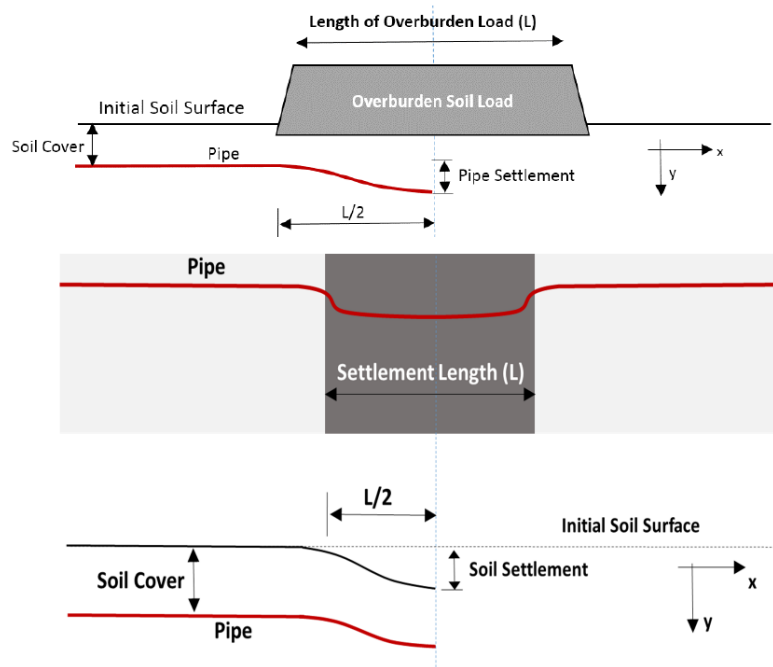
Figure 41 Schematic of pipe deformation due to soil settlement

The nonlinear problem is solved by a step-by-step procedure, with automatic selection of the load step by the program. Equilibrium corrections are applied to compensate for nonlinear effects. A table of stresses and strains at the nodes are printed for each loading sequence. The vertical soil displacement in the analysis was assumed at the surface as shown in Figure 38, with short and large displaced lengths of 60 and 120 ft. The analysis was carried out with soil displacement increments from 12 to 48 inches. Pipe strains and displacements were calculated with the pipe placed 3 ft below the surface. Due to the symmetry, the analysis was carried from joint (1) at -300 ft on the x-axis to half the displaced soil section as shown in figure.

50
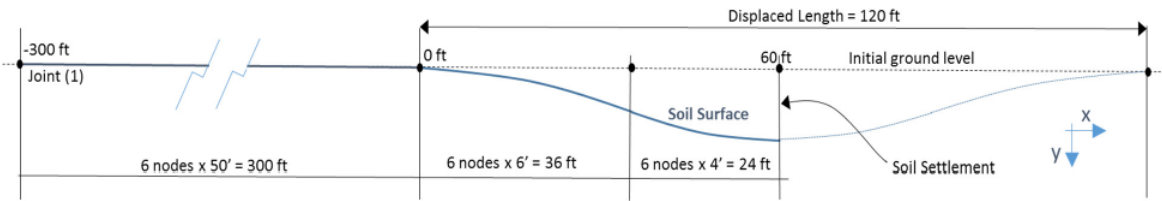
Figure 42 Soil deformation in the FEA analysis

Pipe displacements, hoop, and longitudinal strains were calculated for each increment of soil settlement. An example of the pipe response under vertical soil displacement is shown in Figures 39. The figure shows the FEA results of 4-inch steel pipe buried in sand and clay. The length of the displaced soil section is 60 ft and the figure shows the strain along 330 ft of pipe length to the symmetry line. The plots in the figure represent the axial strains at the bottom of the pipe under incremental vertical soil movements of 24 and 36 inches.
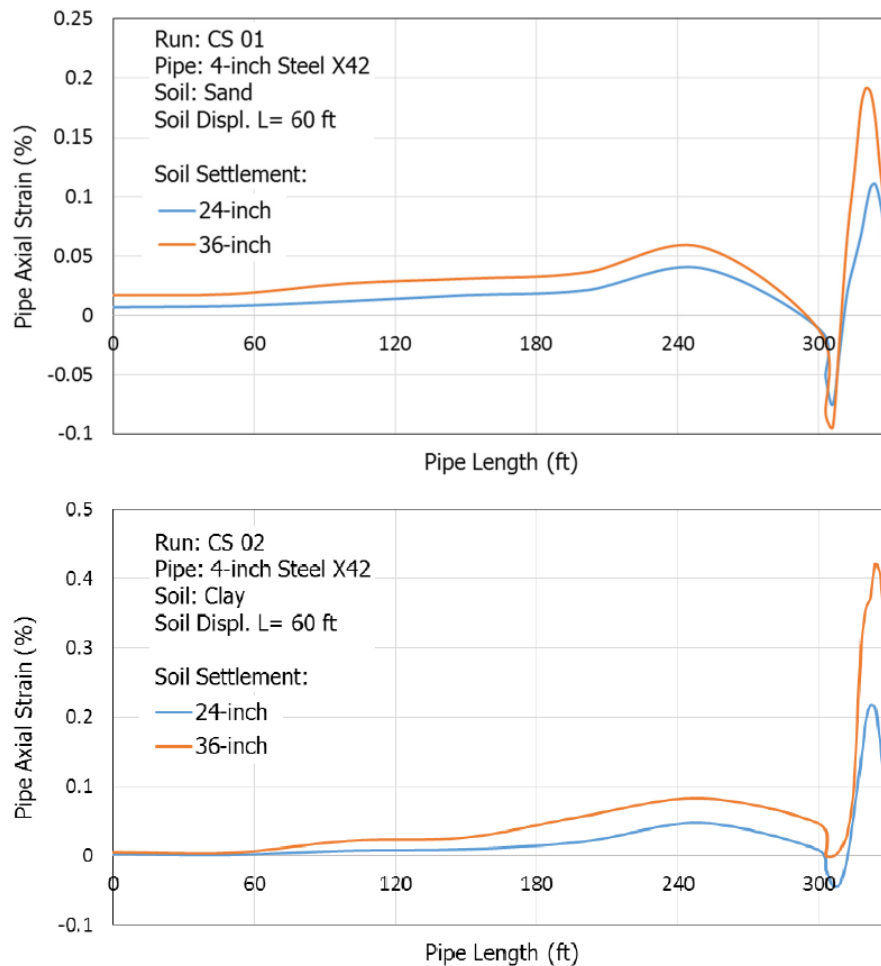
Figure 43 Axial strains at bottom of 4-inch steel pipe in (a) sand, (b) clay

Similarly, Figure 40 shows the axial strains at the bottom of 2-inch plastic (PE) pipe buried in sand and clay. The length of the displaced soil section is 60 ft and the figure shows the strain along the 330 ft of pipe length to the symmetry line. Hoop strains on the plastic pipe for these loading conditions are shown in Figure 41 for the sand and clay soils. Similar to the steel pipe, the plots show higher pipe strains in clay soil.
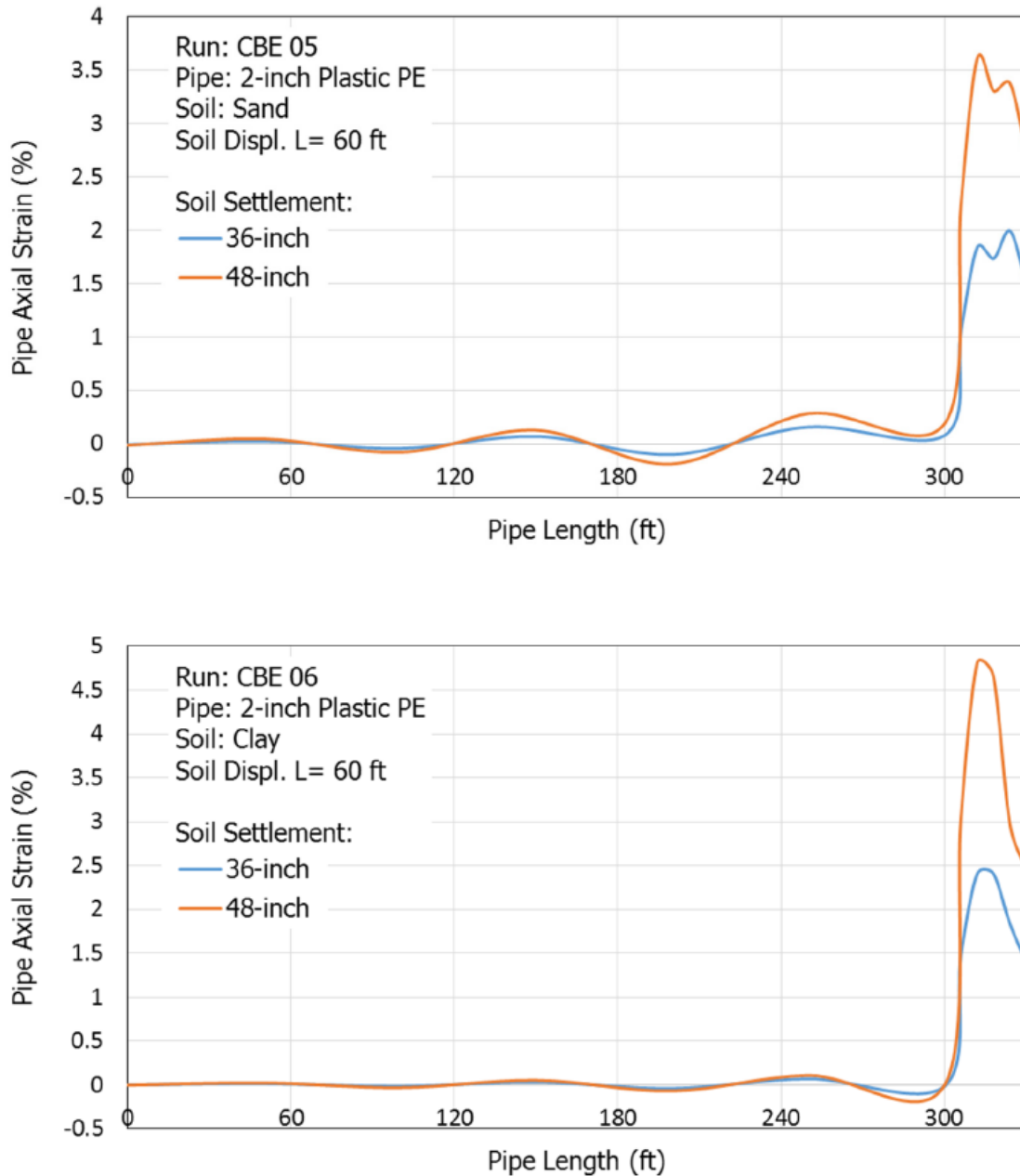
Figure 44 Axial strains at bottom of 2-inch plastic pipe in (a) sand, (b) clay
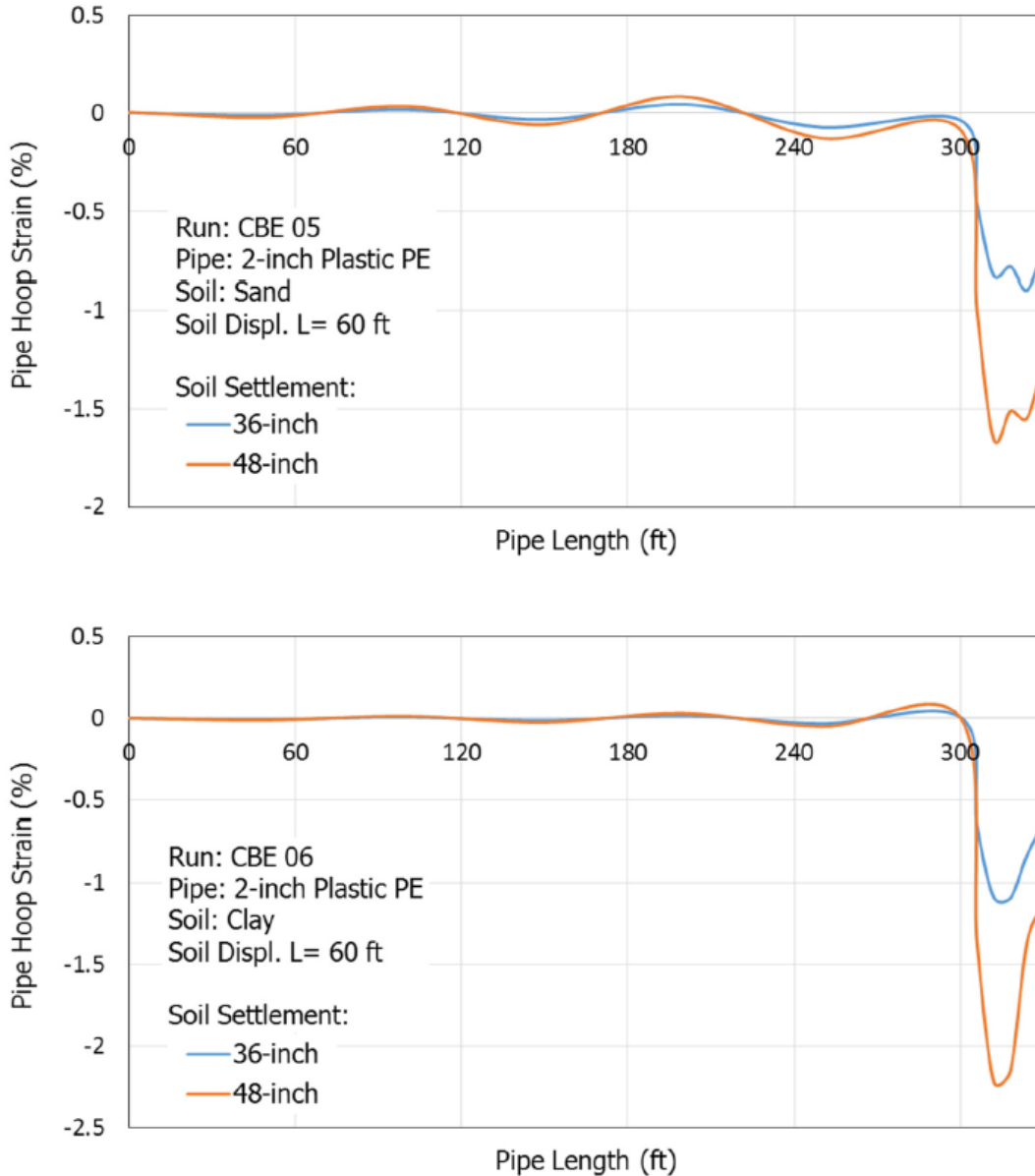
Figure 45 Hoop strains of 2-inch plastic pipe in (a) sand, (b) clay

Figure 42 shows the axial displacement of a 4-inch diameter cast iron pipe in sand under a soil displaced-length of 120 ft and soil settlements of 24 and 36 inches. These displacements are assumed at the pipe joints, which are placed at 12-ft intervals along the pipe. The strength of the cast iron joint plays a significant role in its resistance to pullout due to soil movement. Cement joints (yarn and cement) were the standard joining method by the gas industry in older cast iron pipes. Later joints in larger mains had stronger combination joints of yarn, cement, and lead. Two types of joints were considered in the analysis; namely, weak and strong joints. The properties of

the joints were adopted from an earlier study on thermally induced joint displacements [16] with the weak joints having average pullout capacity of 5 to 25 kips and stiffness of 400 kips/inch.
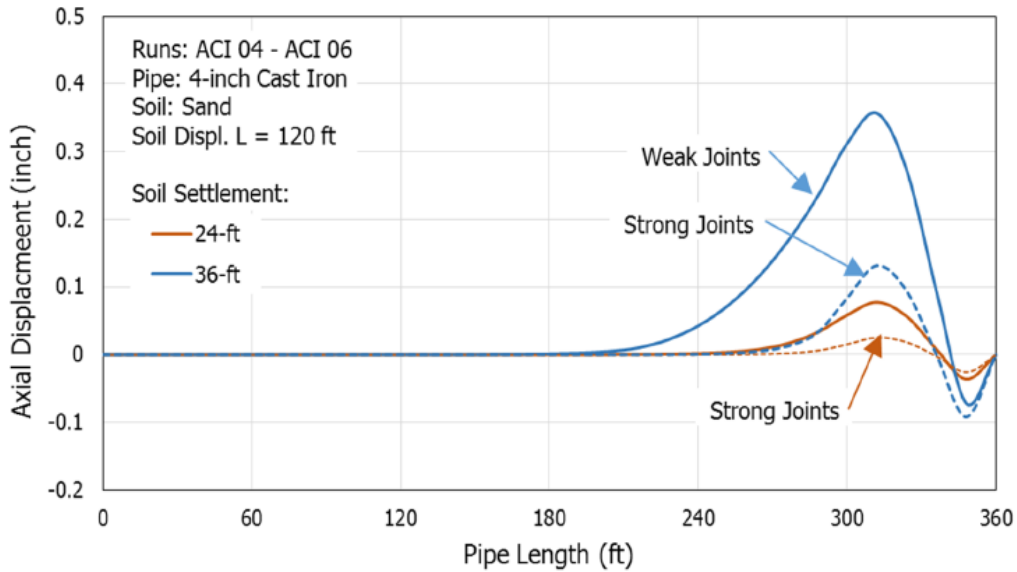
Figure 46 Axial displacements of cast iron joints with weak and strong joints

Horizontal Soil Movement and Landslides

Lateral soil movement and landslides are commonly caused by flooding and heavy rains, and they may result in loss of the lateral support of the pipelines and increased bending or axial stresses. These threats may result in sudden pipe collapse, gas leak, or considerable deformations that induce long-term stresses on the pipe. Figure 43 shows a schematic of pipe deformation under these loads.
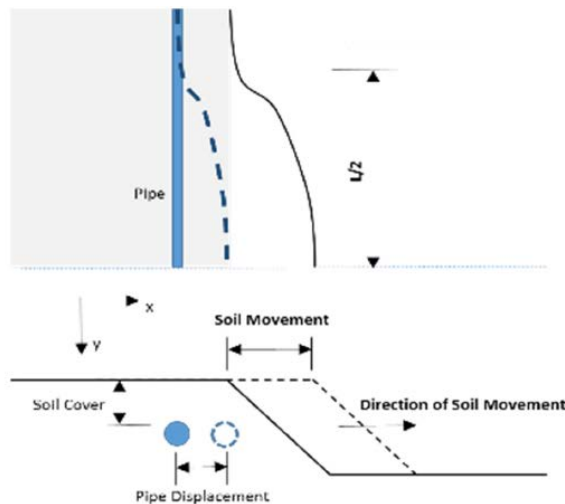
Figure 47 Schematic of pipe deformation from horizontal soil movement

Secondary effects of the earth movement include scour, erosion, and reduced soil cover which may result in higher probability of excavation damage and pipe exposure. Earth movement and landslides are location specific. Pipeline segments in slopes and locations of potential earth movement have high probability of these failure modes. Figure 44 shows the axial strains at the bottom of 2-inch and 4-inch diameter plastic pipes due to horizontal soil movements of 24 and 36 inches and displaced soil length of 60 ft.
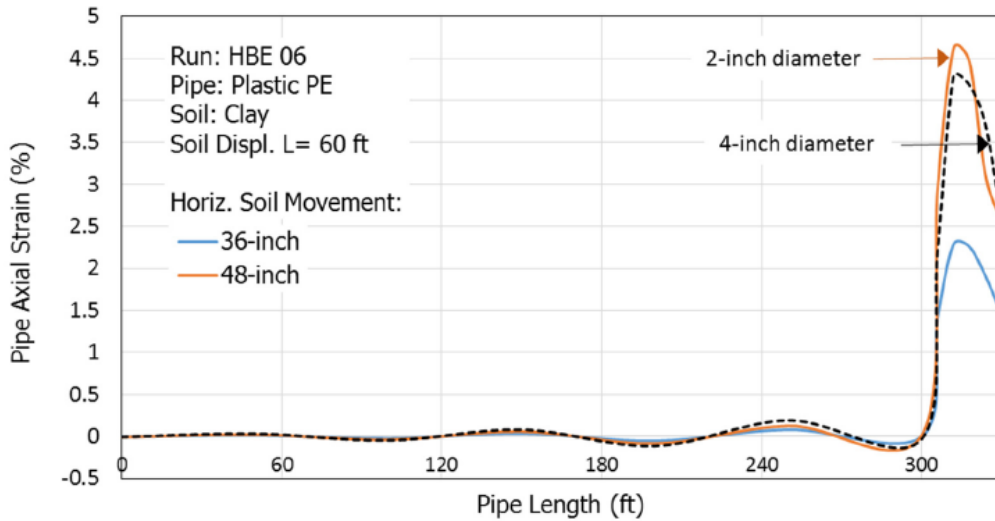
Figure 48 Axial strains in 2-inch and 4-inch plastic pipes

Flooding

Flooding may result in stresses and damage to gas mains and services. Additionally, in low pressure cast iron mains, water may intrude inside the pipe through the joints if the water head above the line is higher than the internal pressure of the pipe. Water levels that cover gas service meters and regulators may also present safety risks. Additionally, heavy rains may expose gas mains and services in areas susceptible to soil erosion; thus subjecting the lines to other threats such as corrosion and excavation damage. The rise of water table in flooded areas can result in a net upward force on the buried pipe when the buoyancy force exceeds the downward weights of the pipe and soil column above the pipe. The largest upward force on a submerged straight pipe per unit length of the pipe can be calculated as [29]:

$$F_b = W_w - [W_p + (\gamma_s h_s - \gamma_w h_w)D$$

Where:

W_w = Weight of water displaced by pipe

55

W_p = Weight of pipe

D = Pipe diameter

γ_s and γ_w = Unit weights of soil and water, respectively, and

h_s and h_w = Height of soil and water above the pipe, respectively.

The bending stress induced in the pipe due to buoyancy σ_b can be approximated by neglecting the resisting soil friction and cohesion at the pipe surface as:

$$\sigma_b = \frac{F_b L^2}{10Z}$$

Where

L = pipe length in the buoyancy zone, and

Z = Pipe cross section modulus (I/D).

The risk factors associated with the uplift load are directly related to the amount of permissible strains resulting from these loads. In cast iron pipes, permissible movements are limited to prevent gas leaks through the joints.

Horizontal Loads on Aboveground Facilities

Horizontal soil and building movements may cause damage to aboveground gas facilities such as regulators and gas meter sets. Figure 45 shows a schematic of the displacement of an aboveground gas meter due to outside horizontal force. Although it is unlikely that wind force will directly damage the aboveground facility; it may blow over a structure such as a tree or fence which may also strike the aboveground pipeline or pull up a belowground pipeline. The risk factors are determined from the permissible movement of the joint before leak occurs, as defined by the subject matter experts and utilities experience. Aboveground deformations are directly quantified and evaluated from direct measurements during walk-in and remote sensing surveys.
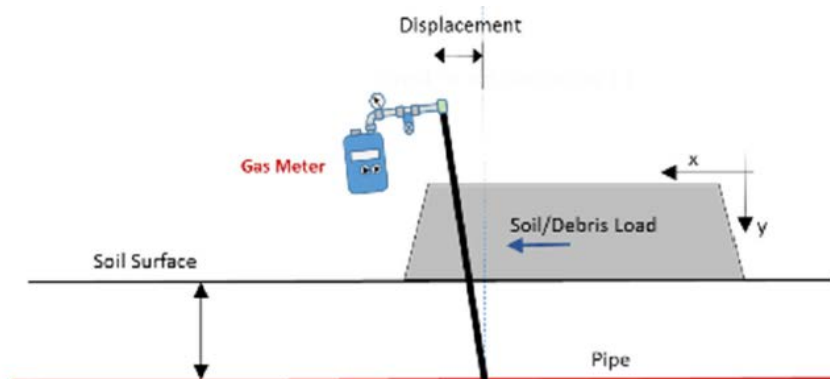
Figure 49 Schematic of displacement of aboveground facility

Acceptable Criteria of Pipe Stresses and Deformation: In post-disaster analysis of pipe risk due to outside force, measurements of pipe displacements, strains, and bending moments are used to determine the risk factors associated with the pipeline types and attributes. The pipe segment attributes which affect its susceptibility to threats from natural disasters are summarized in Table 6.

Table 4 Attributes to the Threats from Nature Disasters

Threat	Asset Type	Influencing Factors
Earth Movement & Landslides	Metallic Mains & services, Plastic Mains & services, Cast Iron mains, Aboveground gas meter sets & regulators.	Area topography and soil type, Pipe vicinity to hazard & orientation Pipe type and size and Age, Joint type.
Flooding	Metallic Mains & services, Plastic Mains & services, Cast Iron mains, Aboveground gas meter sets & regulators.	Area topography and soil type, Pipe vicinity to hazard and soil cover Gas meter height above ground Cast iron Joint type and pressure
Wind and horizontal loads	Aboveground gas Meter sets.	Tornado & hurricane risk areas, Facility's vicinity to hazards, Aboveground facility structure type.

Several studies provide guidelines on the permissible limiting strains of the pipe under outside forces [15, 30]. The American Society of Civil Engineers (ASCE) provides an allowable acceptable criteria defined by loads, stresses deformations or strains for pipelines subjected to outside forces [21]. Table 5 shows suggested criteria for most applications. The American Society of Mechanical Engineers (ASME) also specifies an alternate design of pipes based on strains in situations where the pipeline experiences a predictable noncyclic displacement of its support (e.g., fault movement along the pipeline route or differential subsidence along the line) [22]. It suggests the use of permissible maximum longitudinal strains in place of the longitudinal and combined stress limits for safety against excessive yielding. The permissible maximum longitudinal strain depends on the ductility of the material, previously experience of plastic strain, and the buckling behavior of the pipe. Where plastic strains are anticipated, the pipe eccentricity, pipe out-of-roundness, and the ability of the weld to undergo such strains without detrimental effect should be considered.

Table 5 Suggested Allowable Criteria for Outside Force [21]

Loading Condition	Allowable Load or Stress	Allowable Deformation or Strain
Hoop stress from internal pressure and fluid transients	Code allowable for internal pressure	N/A
Through-wall bending from earth loads (static, live, surface impact)	Bending stress < 0.5 σ_y	N/A
Hoop compression from earth loads (static, live, surface impact)	Compressive stress < 0.5 σ_y	N/A
Ring buckling from earth loads (static, live, surface impact)	Compressive load < $\frac{1}{FS}\sqrt{32 R_W\, B'\, E'\, \frac{EI}{D^3}}$	Strain limits: Mortar-lined and coated = 2% D Mortar-lined & flexible coated = 3% D Flexible lining & coated = 5% D
Bending stress from buoyancy	Bending stress < σ_y [6]	Strain limits: Tension: 0.5% Compression: 0.5%
Thermal expansion	Code allowable for secondary loading [1]	N/A
Movement at bends	Code allowable for primary loading [1]	N/A
Longitudinal strain from ground movement due to earthquake, landslide, or mine subsidence, combined with thermal strain	N/A [2]	**Operable limits [4,5]** Tension strain limit 2% Compression strain limit $0.50\left(\frac{t}{D'}\right)-0.0025+3000\left(\frac{pD}{2Et}\right)^2$ $D' = \dfrac{D}{1-\frac{3}{D}(D-D_{min})}$ **Pressure integrity limits [4,5]** Tension strain limit 4% Compression strain limit $1.76\frac{t}{D}$
Wave propagation [4,5]	Bending stress < σ_y	Tension strain limit 0.5%

Assessment of Pipelines Due to Natural Forces

Strains in Steel Pipes

The results of the FEA of 2-inch and 4-inch diameter grade X42 steel pipes in various soils are compiled in Figure 46. The figure shows the maximum pipe axial strains at the bottom of the pipe at various soil settlements.

58
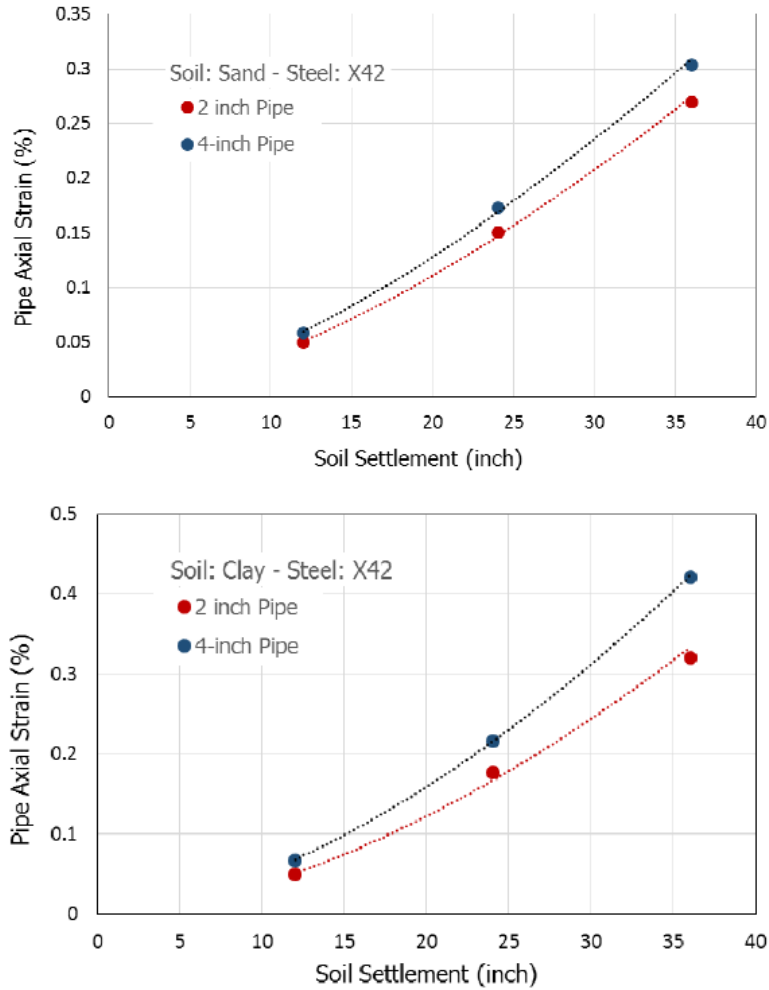
Figure 50 Axial Strains in steel pipes due to soil settlements (a) sand, (b) clay

Strains in Plastic Pipes

The results of the maximum axial strains of various sizes of plastic pipes are shown in Figure 47. The figure shows the strains at various soil settlements of a displaced length of 60 ft. Similar to steel pipes, the results show higher axial strains in clay soil than in sand.
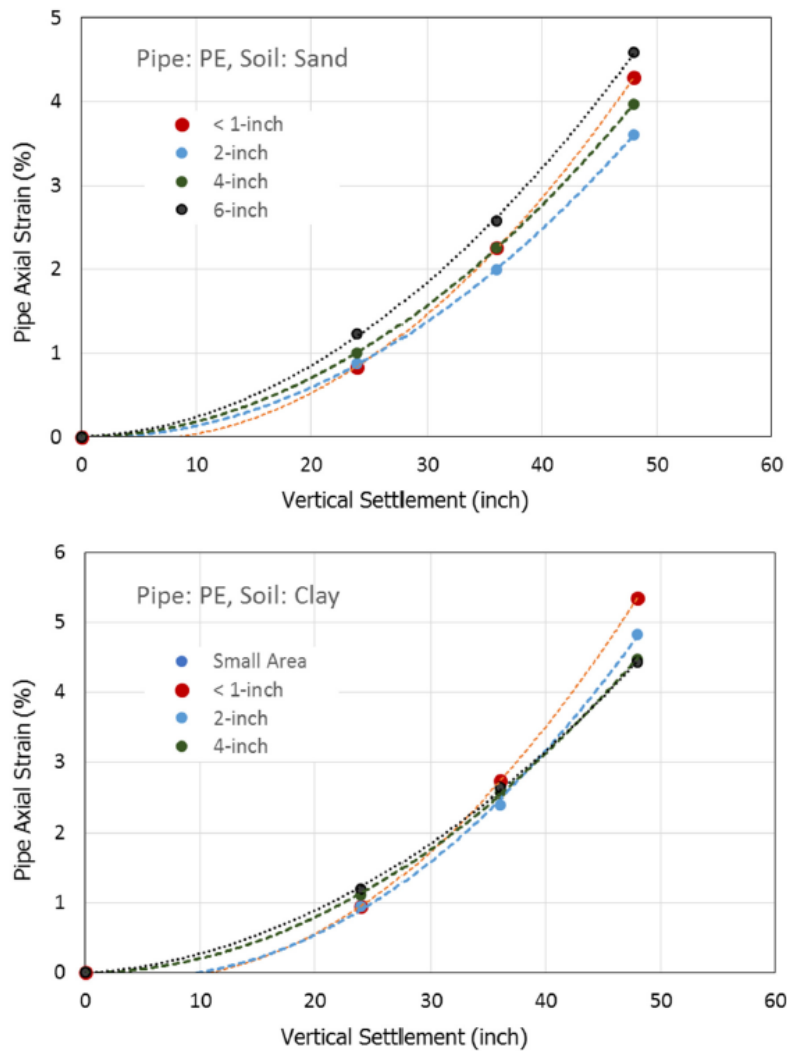
Figure 51 Axial Strains in plastic pipes due to soil settlements (a) sand, (b) clay

Axial Displacement in Cast Iron Pipes

The joint strength of the cast iron pipe plays a significant role in its resistance to pullout due to soil movement. Accordingly, axial deformations at the joints were evaluated for various soil settlements. Figure 48 shows the deformations of strong joints for various pipe sizes in sand at soil settlement length of 120 ft.
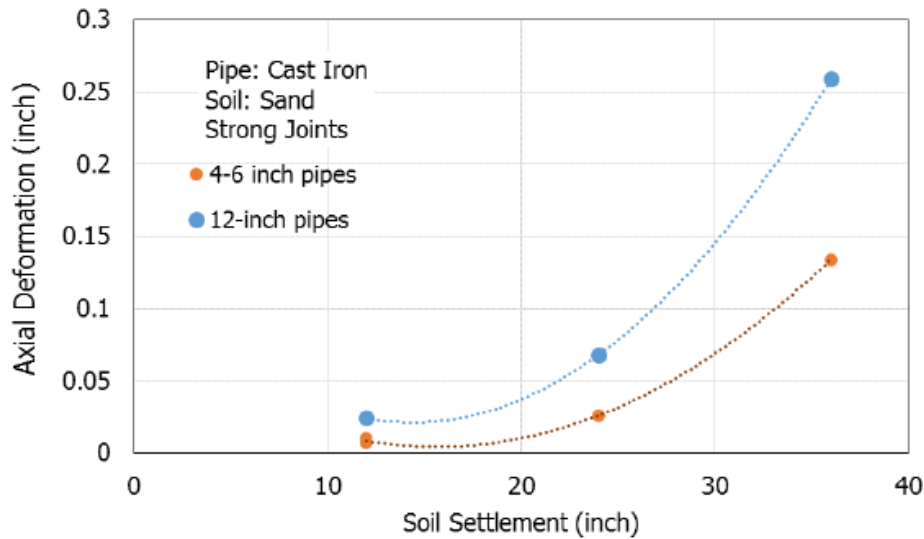
Figure 52 Axial Strains in cast iron due to soil settlements (a) sand, (b) clay

Consequences of Failure (COF)

COF is a measure of the impact of a pipe damage within a structure on the population. The specific expression of this consequence is determined by the operators and will be generally discussed in a later phase of the project. The primary driver for COF is casualties and/or property damage arising from gas entering property from a leak. The three factors which the operators used to quantify COF are:

- Probability of Leak: The likelihood that a component will leak or rupture,
- Probability of Gas Ingress into a Structure: The probability that escaped gas from a leak or rupture will enter a building,
- Probability of Ignition: The probability that gas which has escaped into a structure will ignite.

Event Tree Analysis (ETA) can be used as an inductive technique that allows the user to determine the risk of certain consequences due to different sequences of events. An ETA consists of an initiating event from the Fault Tree analysis (e.g., gas meter damage due to flooding) which is the direct cause of an event, and a series of different consequences. Different combinations of which allow the Initiator to result in consequences.

Bayesian Network Analysis of Likelihood of Damage

Pipeline deformations resulting from soil movements were shown in the previous chapter for various pipe materials, sizes, and soil types. These deformations were combined with

estimates of pipeline damage due to flooding (i.e., likelihood of water intrusion and uplift of large size pipes). These estimates were then weighted based on pipeline age and its previous history of leaks and corrosion potential to produce an overall estimate of its likelihood of damage. A Bayesian Network (BN) approach was used to integrate the above conditions and produce the overall damage probability. The BN approach may be summarized as follows:

- The conditional probability of strains in a pipe segment is initially estimated (e.g., the distribution of pipe axial strains due to vertical soil movement).
- Starting with the initial estimate of pipe strains (identified in BN as the prior strain from a soil movement distribution P(H), a specific soil movement (P(E))) results in a new estimate P(E|H) which is the likelihood of the soil movement (E) to occur with the background knowledge of (H).
- The new pipe strain probability P(H|E) is the new posterior of the event and it is calculated as [18]:

$$P(H|E) = P(E|H)XP(H))/(P(E))$$

In real-world events, where many unknown events are related, all the uncertain variables can be graphically represented as nodes in a Bayesian Network. The 'AgenaRisk" software [31] was used to calculate the conditional probabilities of the damage likelihood based on the probabilities of occurrence of the soil movements and floods events. An example of a BN representation is shown in Figure 49 for a sample problem of plastic pipe damage likelihood resulting from the combined effects of soil movement and flood. The sample problem utilized pipeline data from segment at the coastal area in the State of New Jersey. The figure shows the distributions of pipeline types and sizes based on data compiled from the LDC Company in the area. The distribution of soil types was based on the U.S. Geological Survey data shown in Figure 50 for soils in 7 counties in the coastal area. A normal distribution of the horizontal and vertical soil deformations in the area was assumed for the initial estimation of pipe strains. The damage potential of the plastic pipes is ranked from SME inputs of the pipe history of leaks and potential of excavation damage in segments with inadequate depth of cover.
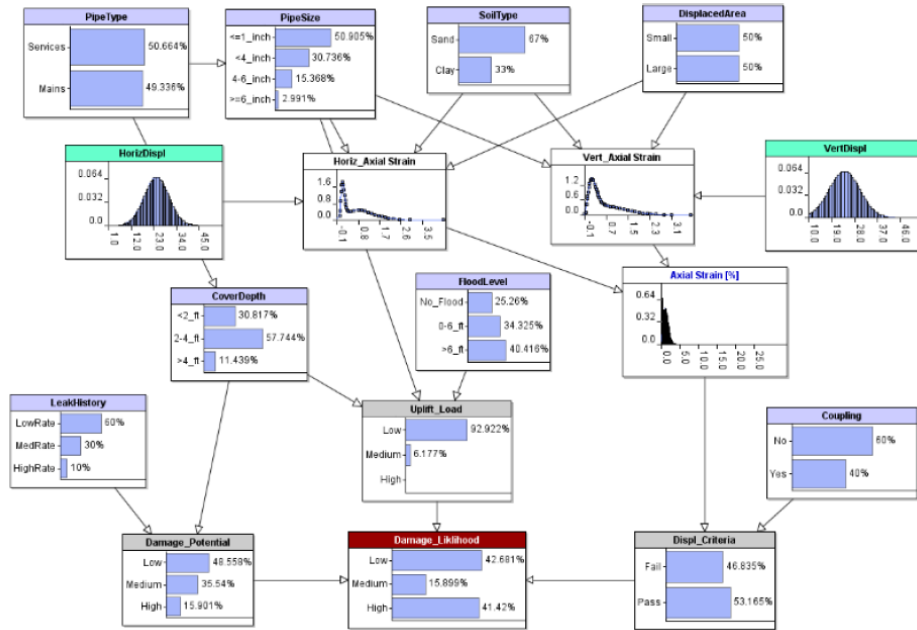
Figure 53 Bayesian network for the plastic pipes probability of damage
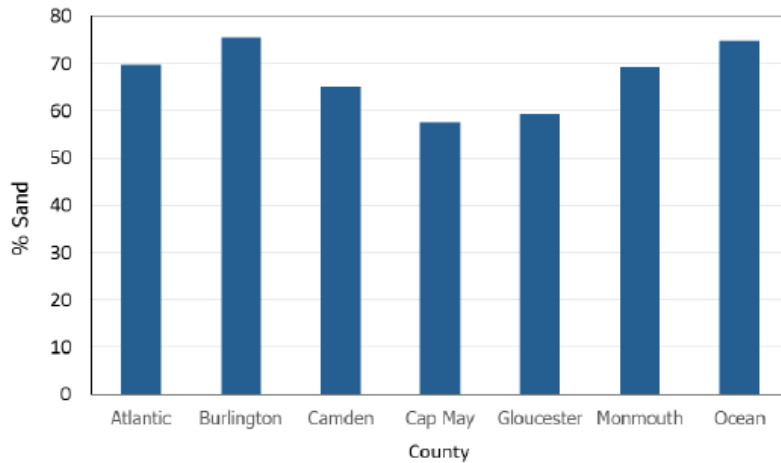
Figure 54 Distribution of sand in the NJ coastal area

Similar BN figures were constructed for the steel and cast iron pipes as shown in Figures 35 and 36, respectively. For steel pipes, the corrosion potential had initial normal distribution. Similarly, the age of the cast iron pipes was assumed to have normal distribution as shown in Figure 34, based on data from LDC companies at the east coast.
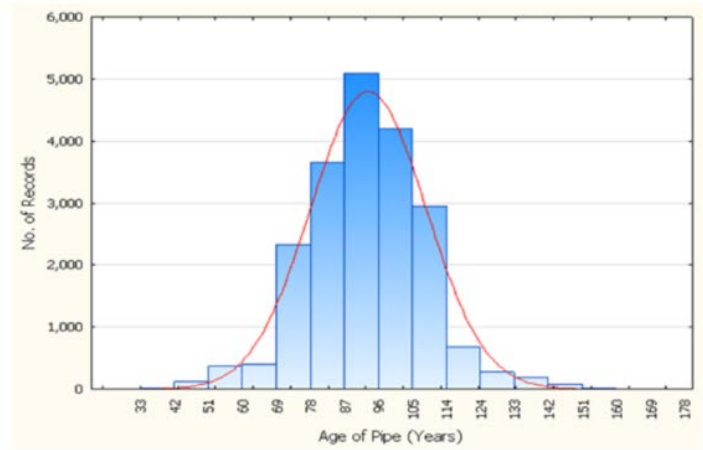
Figure 55 Distribution of ages of cast iron pipes in the east coast LDC's
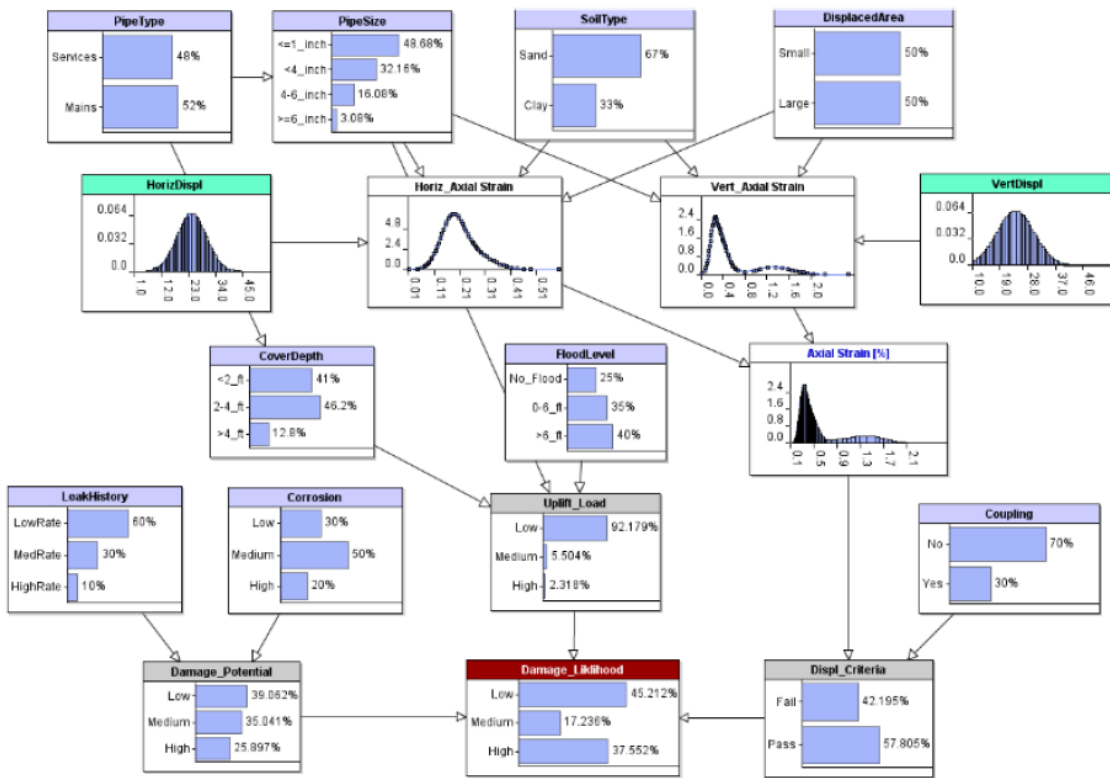
Figure 56 Bayesian network for the steel pipes probability of damage
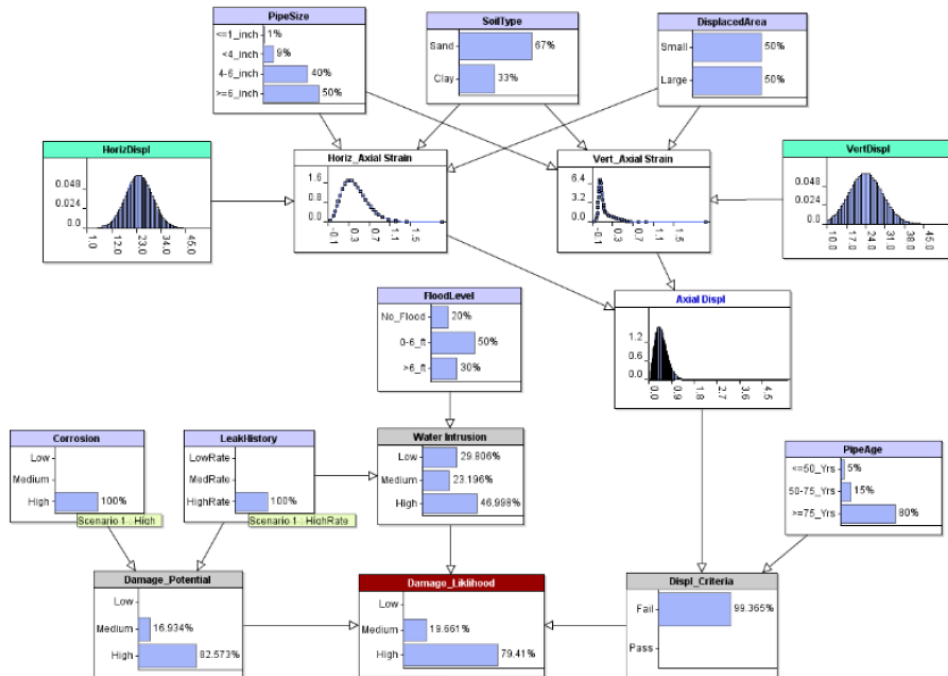
Figure 57 Bayesian network for the cast iron pipes probability of damage

After the damage estimates are established from the initial distributions of the BN network, pipe parameters and post-damage characteristics are used in the program to estimate the associated likelihood of damage. An example of this procedure is shown in Figure 38 for the plastic pipes with the following input data:

- Pipe size: 2 inch,

- Soil type: Sand

- Horizontal displacement: 0 inch

- Vertical displacement 24 inches, for a displaced length longer than 120 ft (i.e., long displaced pipe segment)

- Depth of cover: 3 ft

- Flood level: 0-6 ft

- Leak history: Low rate

- Joint coupling: No mechanical couplings

The damage likelihood under these parameters changed from its initial values shown in Figure 54 and Figure 55-(a) to a low damage likelihood as shown in Figure 55-(b) for the parameters in the above example. A decrease of the length of the displaced soil results in a significant increase of pipe strains. This is demonstrated in the run shown in Figure 56 with a

short length of the displaced soil, while keeping the other parameters unchanged. The damage likelihood in this case is shown in Figure 55-(c).

(a)   (b),   (c)
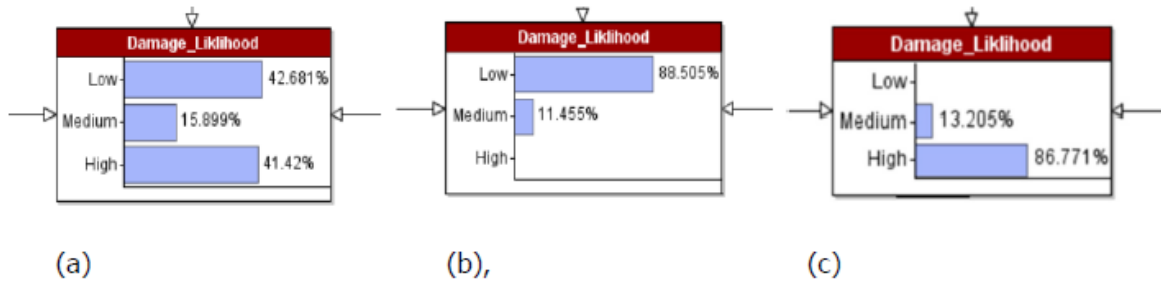
Figure 58 Damage Likelihood for (a) initial estimates, (b) Long displaced section, (c) short displaced section
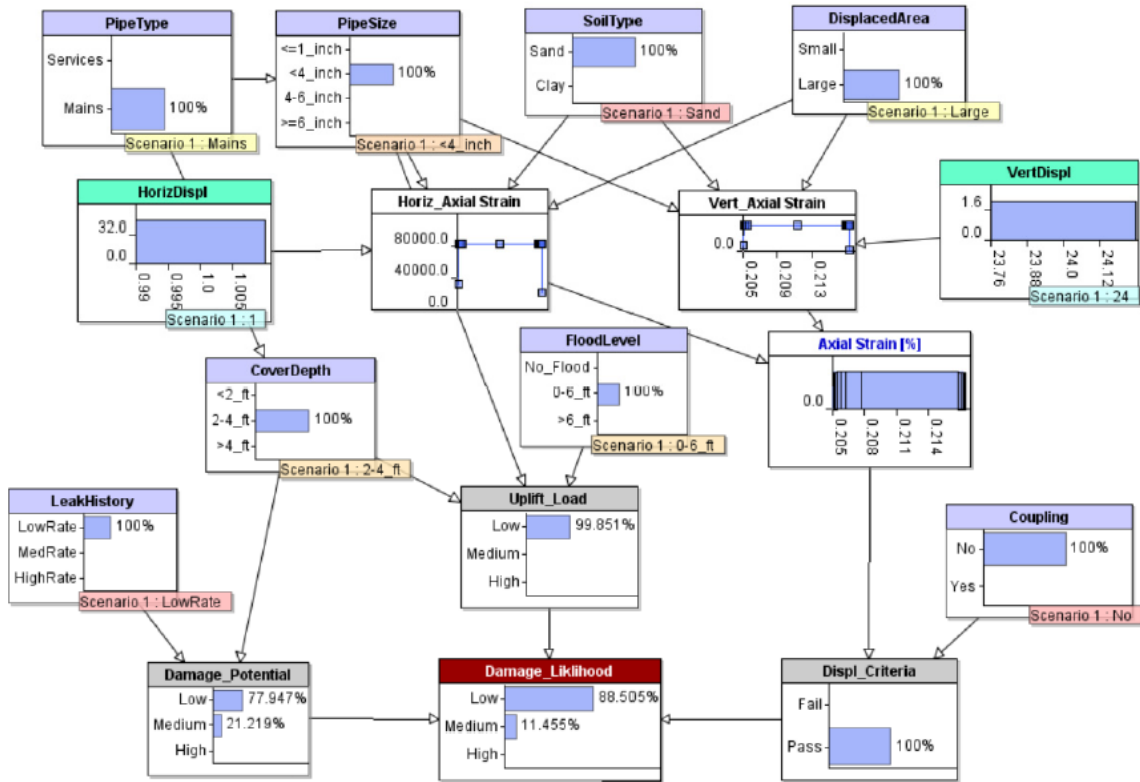
Figure 59 Example of BN for the plastic pipes with large displaced length
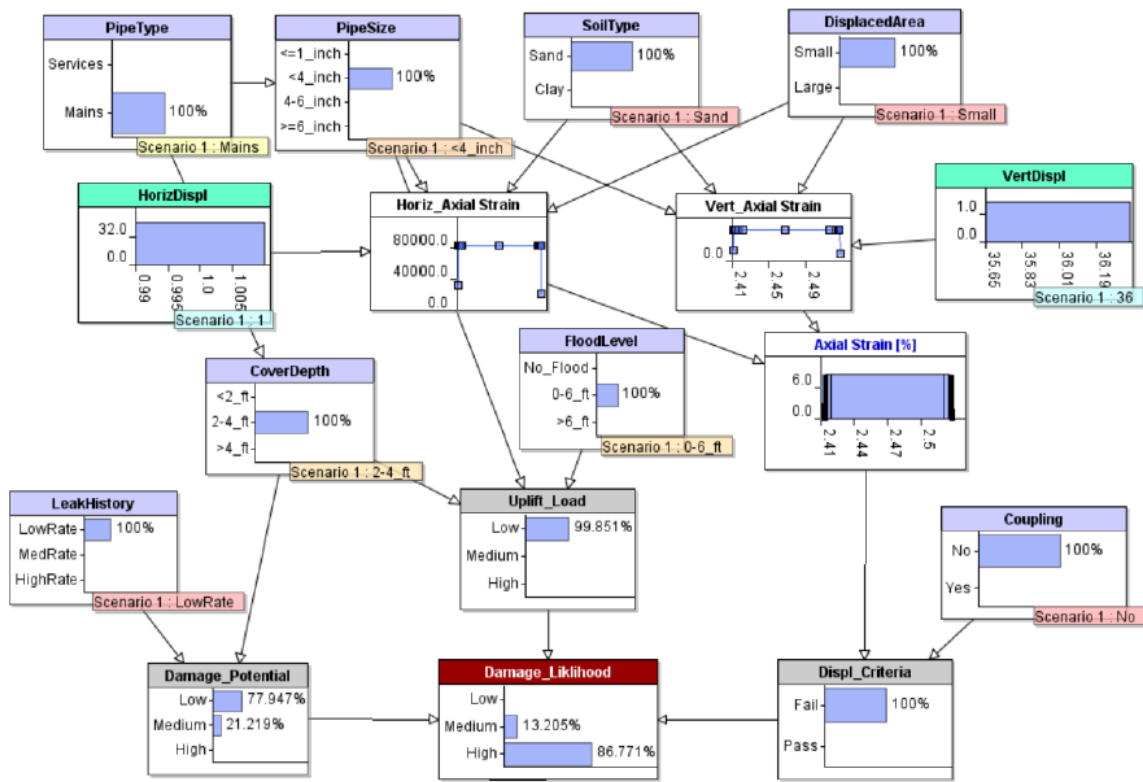
Figure 60 Example of BN for the plastic pipes with small displaced length

Web-Based Program for Pipeline Risk Due to Natural Forces

Program Login

The web-based program 'Pipe Assess' provides an estimate of the damage probability of belowground natural gas distribution pipelines due to natural forces threats. The assessment of risks due to natural forces are calculated for the following threats:

- Horizontal and vertical earth movement,
- Static water table resulting from flooding.

These threats may result in sudden pipe collapse, gas leak, or considerable deformations that induce long-term stresses on the belowground pipeline. The program is accessed at the following web-page address:

http://gasapps.gastechnology.org/pipeassess

The user enters the 'User Name' and 'Password' in the login page shown in Figure 57. The program is available to the users who have access to this report by using the User Name: pipeuser and the Password: piperisk.

67

Figure 61 Pipe Assessment Program login page

Program Example

Figure 58 shows the data entry page for an example of the assessment of a PE main pipe segment with the properties shown in figure. The pipe is buried in 3-ft of sand cover with 24 inches of soil vertical displacement. The results in Figure 59 show a low probability of pipe damage of about 8% due to the soil movement. The results in Figure 60 show a significant increase in the pipe damage likelihood when the soil vertical displacement increases to 36 inches and with unknown knowledge of mechanical couplings in the line (i.e. a probability of 50% of having mechanical couplings in the line).

Figure 62 Data entry for an example of a PE main pipe

Figure 63 Results of the PE data entry example

69
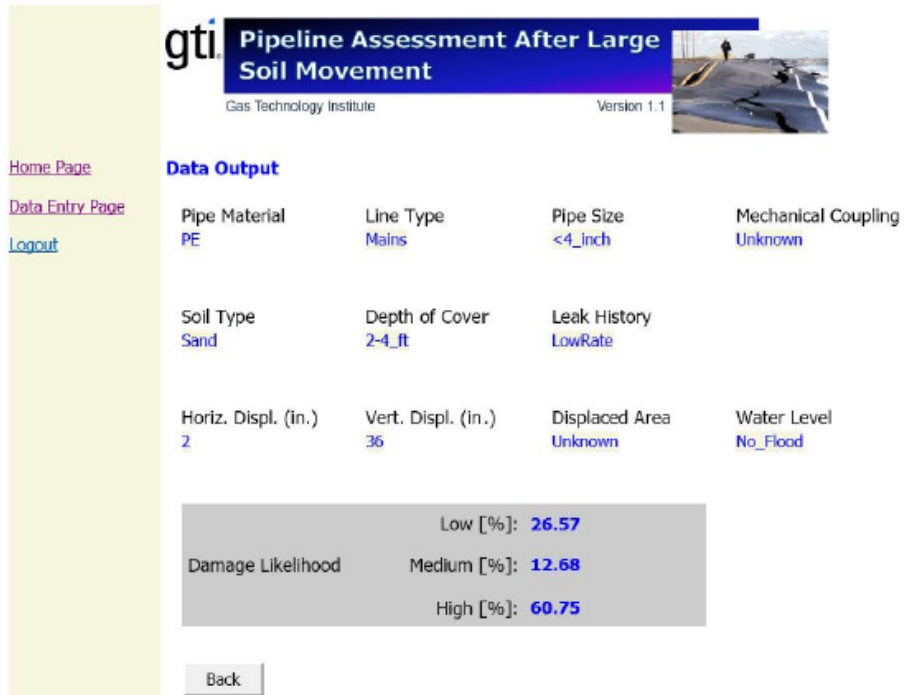
Figure 64 Increase in the damage likelihood in higher soil displacement

GIS-based Risk Assessment Program

In addition to the online portal for risk assessment, the research team also developed an ArcGIS based risk assessment module. The ArcGIS based program can take spatially distributed threat information in the format of shapefile and run above-ground and below ground damage assessment for the network wide gas distribution system. The following figure shows the input of threat information (Figure 65a), the loading of pipeline network (Figure 65b), and computing of damage likelihood based the risk assessment approach illustrated above (Figure 65c).
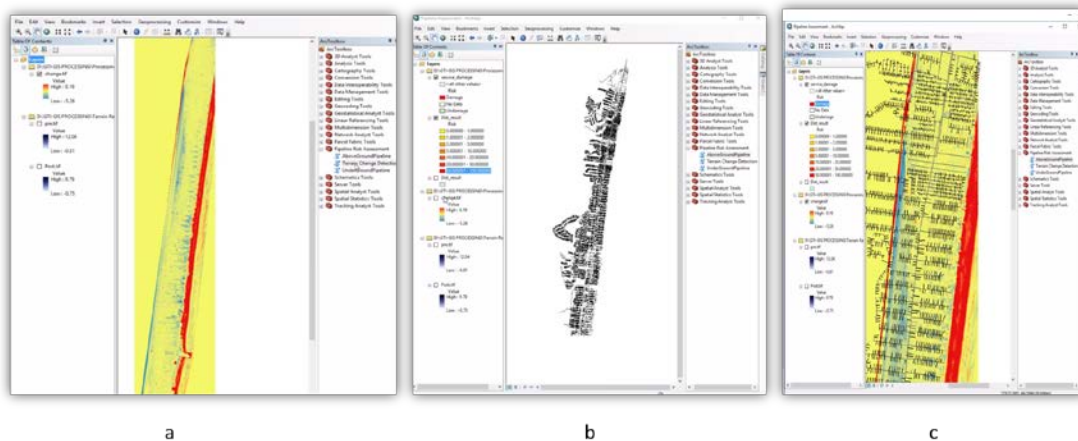
Figure 65 GIS-based Pipeline Damage Assessment Module

70

Case Study - GIS Mapping of Post-Disaster Areas

A post-disaster risk assessment of natural gas pipes was performed in a case study of the pipeline system in the east coast after hurricane Sandy. The study area is about 3 miles long and 0.5 wide at Ortley Beach in New Jersey. Figure 47 shows the study area. The area was divided to two sections; namely A and B to allow for a detailed display. A GPS map of the natural gas distribution system of the area was obtained to identify the grids containing the pipeline system. Figure 48 shows the pipeline system in Area B. The pipeline attributes of this system (e.g.; pipe type and size) were used in the web-based program Pipe Asses along with the hurricane Sandy post-disaster data to provide an estimate of the damage likelihood of the pipe segments.

Figure 66 A view of the coastal study area in NJ
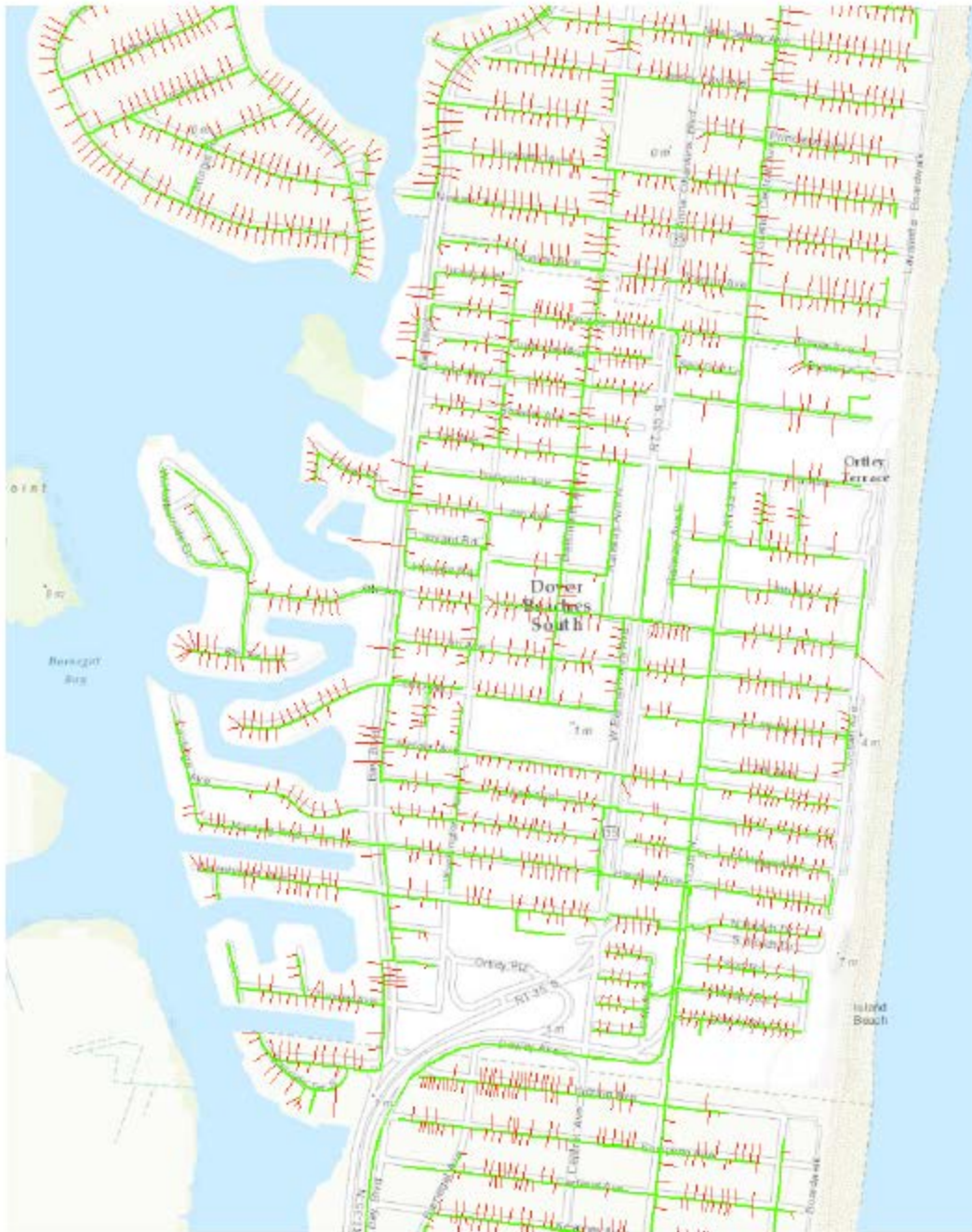
Figure 67 Natural gas pipeline system in Area B of the study

The soil types and properties in the area were obtained from the Web Soil Survey data [32]. The post-disaster soil deformations were provided by the Rutgers University based on their mobile hybrid LiDAR data after hurricane Sandy. Figure 63 shows the soil displacements, calculated from the pre- and post-disaster LiDAR soil elevations. The displacements are displayed on the GPS pipeline grids in the figure.

The changes of the water elevations after hurricane Sandy were obtained from the Federal Emergency Management Agency (EMA) data and are shown in the GPS map in Figure 50.

Figure 68 Soil displacements after hurricane Sandy in the study area

Figure 69 Water elevations after hurricane Sandy in the study area

The grid areas containing the natural gas mains and subjected to soil movement and flooding were analyzed. The analysis incorporated the pipe properties, soil displacement, and water elevations in the Pipe Access web-based program. The results of the likelihoods of failures

74

of the mains are shown in Figure 65. The ranking level of 'High' in the figure corresponds to more than 50% likelihood of failure of in the program output.

Figure 70 Likelihood of failures of belowground pipes in Area B

CHAPTER 5. INDUSTRY INVOLVEMENT, OUTREACH, AND IMPLEMENTATION

Throughout the project, a group of technical advisory stakeholders has provided valuable inputs to the project development (Table 6). We have engaged this group through conference calls, face-to-face meetings, and workshops. The following table (Table 7) provided a summary of technical advisory committee activities. Of particular note is that we have conducted an online survey with this group of stakeholders and other major utility companies. Details of the survey form and results can be found in APPENDIX B.

Table 6 Technical Advisory Stakeholder Members

Technical Advisory Stakeholders	Company/Agency
James Merritt	UDOT Pipeline Safety
Mary Holzmann	National Grid
Steven Hope	NYSEG
Carrie Berard	NYSEG
George Ragula	PSEG
Ralph E. Terrell	Teco Energy
Richard Trieste	ConED

Table 7 A Summary of Technical Advisory Committee Activities

Quarter	Activities	Agenda
1	TAC conference call	Introduction of project members and project objectives
2	Online Survey of TAC members and other affiliated companies	
3	TAC conference call	Discussion of survey results
4	TAC face to face meeting and conference call	Reporting project progress and system integration results
5	Presentation to TRB utility committee	Reporting project progress and results
6	Presentation at OKC CRS&SI workshop and presentation to the co-funding utilities in the OTD program.	Reporting project progress and results
7	Presentation to the co-funding utilities in the OTD program.	Seeking inputs from natural gas facility stakeholders on the utility of our developed methodology
8	Presentation to the co-funding utilities in the OTD program & OTD newsletter	Reporting project progress and seeking stakeholder opinion on developed tools
9	Presentation to the co-funding utilities in the OTD program	Reporting project progress and seeking stakeholder opinion on developed tools
10	TAC activities integrated into the Mini-Workshop on Remote Sensing Technologies for Post-Disaster Risk Assessment of Natural Gas Pipeline Systems	System demonstration and user feedback

In addition to regular meetings with the industry advisory committee, the research team has also focused on dissemination of the research results through conference presentations, system demonstrations, and workshops. Table 8 provides a summary of demonstration and technology transfer activities.

Table 8 A Summary of Demonstration and Technology Transfer Activities

Date	Name	Type	Location
March 29, 2015	A presentation at the Society of Gas Operators	Presentation	New York City
May 14, 2015	System demonstration and research presentation to Mr. Winfree's staff members	Demonstration and Presentation	Rutgers CAIT
June 3, 2015	System demonstration to Mr. Caesar Singh, the program manager of CRS&SI research program	Demonstration	Rutgers
November 3, 2015	Visions for the Future Forum at the 2015 Bentley Year in Infrastructure conference	Presentation	London, United Kingdom
December 22, 2015	Research presentation at the NSF Prism Lecture Series at City University of New York	Presentation	New York City
Jan, 2016	TRB Workshop 160 - Sensing Technologies for Transportation Applications Multi-Source Remote Sensing Data Fusion for Post-Disaster Assessment of Natural Gas Pipeline Systems	Presentation	
Jan, 2016	Session 428 – Hazardous Materials Transportation Research Risk Analysis of Natural Gas Distribution Lines Subjected to Natural Forces	Presentation	
Jan, 2016	Session 859 – Advances in Geospatial Technology Applications in Transportation Multiresolution Change Analysis Framework for Post-Disaster Natural Gas Pipeline Risk Assessment	Presentation	
April 13, 2015	Presentation at SPAR Conference	Presentation	Houston
October 28, 2015	NJDOT Research Showcase	Presentation	Trenton
2016	Farrag, K. and Gong, J. (2016) "Risk Analysis of Natural Gas Distribution Lines Subjected to Natural Forces" Submitted to 2016 Transportation Research Board meeting.	Conference Publication	
2016	Zhou, Z., Gong, J., Roda, A., Farrag, K. (2016) "A Multi-Resolution Change Analysis Framework for Post-Disaster Natural Gas Pipeline Risk Assessment" Submitted to 2016 Transportation Research Board meeting.	Conference Publication	
2016	Zhou, Z., Gong, J., Roda, A., Farrag, K. (2016) "A Multi-Resolution 7Change Analysis Framework for Post-Disaster Natural Gas Pipeline Risk Assessment" Journal of Transportation Record	Journal Publication	
May, 2016	Presentations at Cape May UAS in Emergency Response Conference		
June, 2016	Presentation at the Mini-Workshop on Remote Sensing Technologies for Post-Disaster Risk Assessment of Natural Gas Pipeline Systems		

In addition to the presentations and publications, we have also filed A Notice of Invention with Rutgers Office of Research and Economic Development. We are currently in the process of seeking patents on the developed system. At the end of this project, we hosted a half-day workshop at the Rutgers to demonstrate the developed system and software packages to a group of stakeholders including utility owners, regulatory agencies, and UAS startup companies (Figure 67). The workshop was a very successful event. The workshop attendees were particularly interested in the demonstration part. There were great questions and discussions regarding the role of remote sensing, in particular the lidar technology, in assessing the integrity of natural gas pipeline systems. Some particular interesting future research needs that were brought up by the workshop attendees include the ability of using remote sensing to determine the accessibility of critical valves after major disasters and the role of remote sensing in locating buried assets after major topological changes as the results of disaster impacts. Some workshop attendees are interested in deploying our systems in monitoring the threat posed by flood to natural gas pipeline systems that are close to rivers and lakes. Further discussions are still ongoing with these companies in terms of establishing service provider agreement. Detailed meeting minutes and agenda can be found in Appendix D.

During the course of the project, all the required quarterly reports have been submitted on time. For each quarter, we also have created newsletters. Detailed information can be found at http://cait.rutgers.edu/pssp/monitoring.

As part of the implementation plan task, the research team has conducted market analysis of gas pipeline inspection methods, and investigated how current geospatial products are used in gas operators' in-house programs. This leads to the development of a business process model on how the developed technologies can be conveniently integrated into utility owners' existing process. We found risk assessment is an essential element in the natural gas industry. Most of the above risk assessment approaches require high quality data in order to be useful. During large-scale extreme events, there is a need for approaches that can rapidly synthesize information and condition data and feed these information into the risk assessment framework. Remote sensing is an effective method for gathering threat information in large areas. However, it seems little integration in these two domains has been achieved. Integration of remote sensing data into the risk assessment frameworks is of great need for gas operators.

Figure 71 Remote Sensing Workshop

To facilitate remote sensing based risk assessment, it is important to realize that a distributed approach would be necessary. This is due to several reasons: (1) most gas operators do not collect remote sensing data by their own; instead, they use publicly available data or hire contractors to do so; (2) most gas operators are reluctant to share data about the location and conditions of their assets as they are deemed sensitive: and (3) natural disasters are rare, meaning it is not economic for them to own software packages that can integrate remote sensing data and risk assessment models. Based on these observations, what we proposed is a distributed and cloud based business model (Figure 67). The workflow we proposed is: the software packages are divided into two components: Web-based risk assessment model and a standalone software

package that deals with processing collected remote sensing data and detect hazardous conditions posing threat to the natural gas pipeline system. Once a natural disaster strikes, the gas operator choose the region of impact for analysis. The threat detection software gathers and processes available remote sensing data and detects salient threats. The geospatially referenced threat data are then extracted and sent back to gas operators. This step does not need detailed information about the locations and conditions of gas infrastructure assets. Then the gas operators upload encrypted gas facility data (through shuffling the data) and their relevant geospatially referenced threat information to the web-based risk assessment program to estimate spatially registered risk on their pipeline segments. This framework would not require the gas operators to purchase the risk assessment program and the threat detection program but only pay as you use. In the same time, it avoids the issue of exposing sensitive pipeline data to the third party.
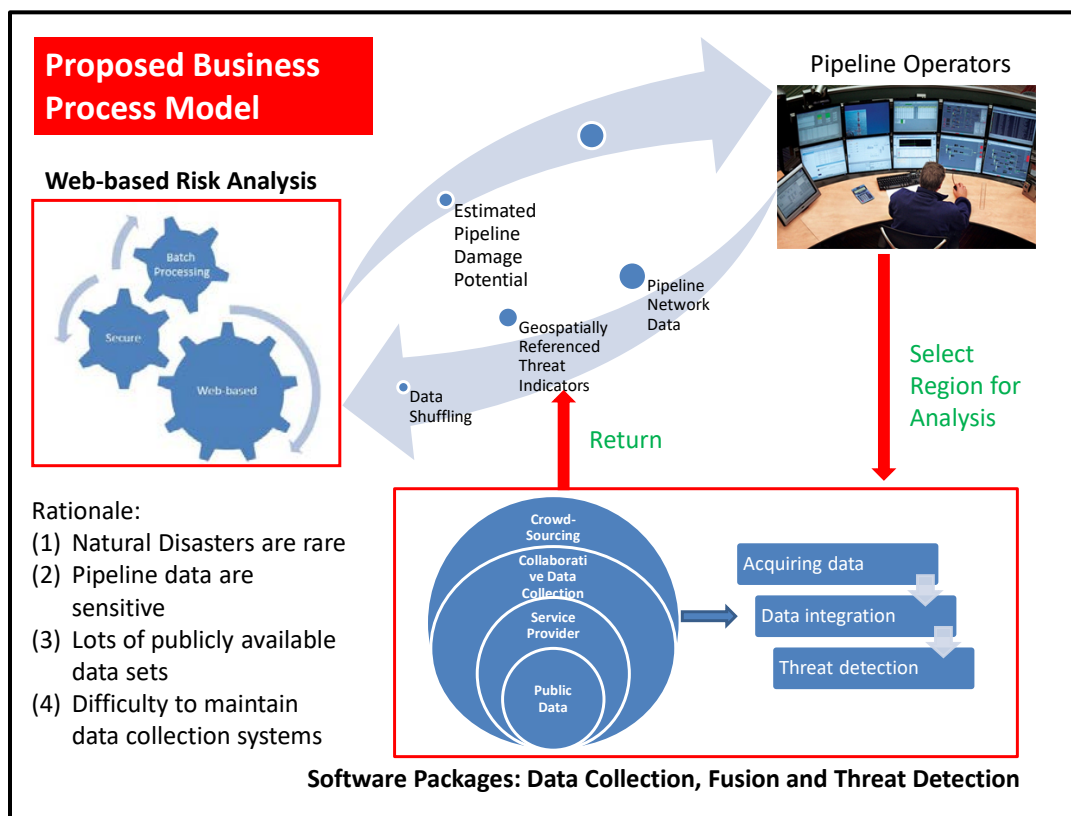
Figure 72 Proposed Business Model

The implementation activities have also been conducted on several fronts: (1) we leveraged the workshop as a platform to engage utility owners and service providers. We invited utility owners in the Northeast region to attend a workshop at Rutgers. They include all the major players

in the state of New Jersey and New York. We also invited UAS startup companies such as American Aerospace to explore partnership in licensing our developed software and hardware systems; (2) we continue to deploy the developed system in several spinoff projects including a FEMA funded Rebuilding for Greater Resiliency project and several bridge and tunnel inspection projects (see below pictures); (3) we have met with Rutgers commercialization office to further our patent application; and (4) we are exploring establish a startup company based on the research products.

Figure 73 FEMA Rebuild for Greater Resilience Project
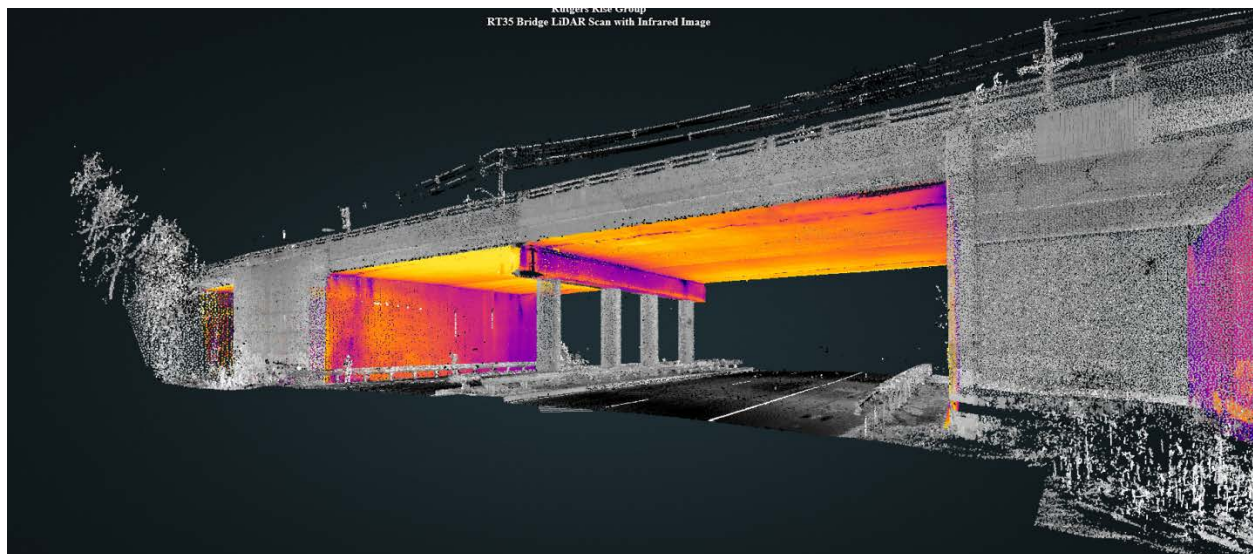
Figure 74 NJDOT Bridge Resource Program
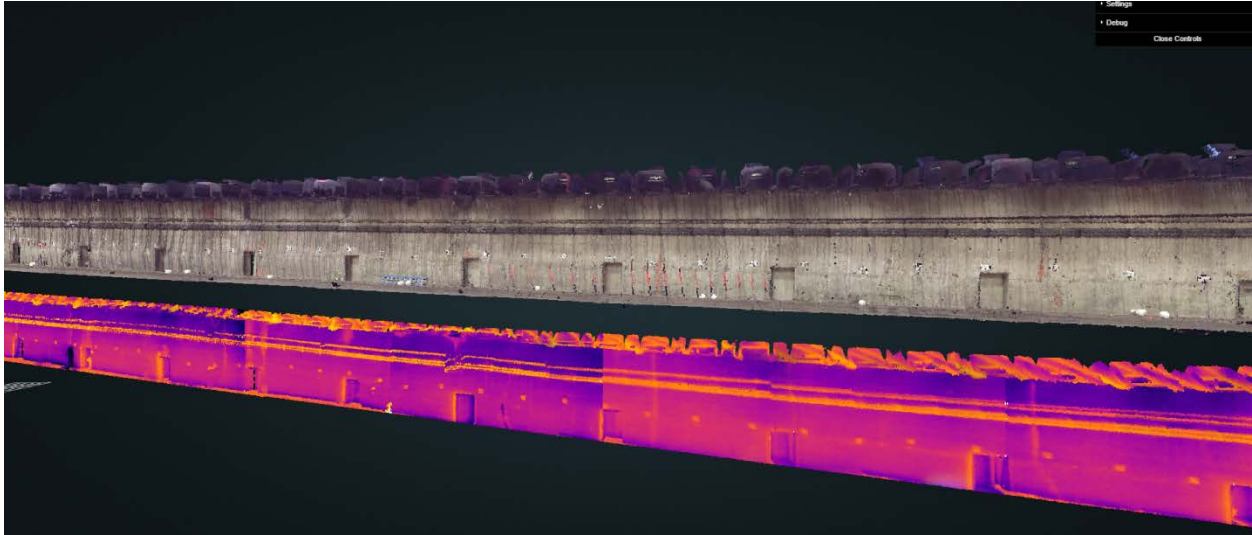
Figure 75 Tunnel Inspection Project in California

No major problems were encountered in this research. The team anticipated a complex data analysis and management process and scheduled into the work plan adequate time for accomplishing milestones. While most of these milestones have been met, two facts have motivated us to request for a 6-month no-cost extension. First, additional time would significantly benefit the refinement of hardware systems and software packages. Robust systems and software packages would significantly increase the potential for successful commercialization. At the time of writing, the team has accomplished the integration and development of a mobile hybrid LiDAR and Infrared Sensing system. The system has been deployed to collect data in various coastal areas for performance evaluation. The point cloud and infrared imagery analysis system and GIS-based pipeline risk assessment tools are under full-swing development. Second, with the recent approval of Rutgers University as a designated Federal Aviation Administration (FAA) Unmanned Aircraft Systems (UAS) testing site, adding a UAS component into this project is cost effective and will significantly expand the utility of our proposed tools. With this in mind, we expanded the capability of the originally proposed point cloud and infrared imagery analysis system and the GIS-based pipeline risk assessment tool such that they can seamlessly integrate UAS-borne imagery and 3D data into the proposed threat detection framework and GIS-based risk analysis tools. At the end of this project, the system is fully functional and has been deployed in various other research projects. This fully demonstrated the impact of this project.

CHAPTER 6. FINDINGS AND CONCLUSIONS

This project is a 30-month journey to develop exciting new geo-capabilities in collecting necessary geospatial data and turning these data into critical tools for rapid assessment of the integrity of natural gas pipeline systems. The research team has met all the goals of the research proposal.

First, the research team successfully developed a hybrid mobile lidar and infrared system that can scan utility infrastructures, more specifically natural gas utility infrastructure, and their surrounding environment at travel speed. The system is fully functional and has been deployed in many critical project scenarios to collect data relevant to risk mitigation and disaster prevention.

Second, the research team developed a threat detection software programs that can fuse multi-sourced geospatial data, whether it is data from airborne or mobile lidar, and detect and quantify threats to natural gas pipeline systems. The program is capable of providing quick visualization capabilities in a web browser environment, gathering necessary data, and processing data into critical insights into threats.

Lastly, the research team developed a web-based and GIS-based risk assessment and visualization system for detecting, ranking, and visualizing high risk pipeline segments based on threat information inputs. The system integrated pipeline mechanistic models, existing pipeline risk models, and remote sensing data into a streamlined tool for wide-area assessment of natural gas pipeline systems following major hurricane events.

We have carefully designed the above three components into a workflow that matches utility owners' business and operation processes. The methodology developed in this project was repeated refined based on inputs from the technical advisory stakeholder groups. Their feedback and support, in some case such as providing testing facilities, have made this project possible. During the course of the project, the research team has made many presentations to the relevant professional society. The project has been highlighted in several issues of Rutgers CAIT newsletters. We have already published one journal paper and two conference papers based on this research, with three more journal papers and one more conference papers in the final stage of the preparation.

We are currently seeking patents for the project products including the hardware system and the software components. The hardware system has been named as SPIRIT (SPatIally Resolved Infrared Thermography). We are also currently seeking establishing a resource center for several gas utility companies and for New Jersey Board of Public Utility. The resource center will focus on implementing and deploying the products out of this research into their operations.

REFERENCES

1. Gas Facts, Annual Statistics, Distribution and Transmission Miles of Pipeline, American Gas Association (AGA), 2015.
2. U.S. DOT, Pipeline and Hazardous Materials Safety Administration (PHMSA), Significant Pipelines Incidents, 2015, http://primis.phmsa.dot.gov/comm/reports/safety/sigpsi.html#_ngdistrib
3. U.S. DOT, PHMSA, Annual Report Data from Gas Distribution Operators, 2014, http://www.phmsa.dot.gov/pipeline/library/data-stats
4. U.S. DOT PHMSA, Gas Distribution Integrity Management Program, http://primis.phmsa.dot.gov/dimp/perfmeasures.htm
5. 49 CFR Part 192, Pipeline Safety: Integrity Management Program for Gas Distribution Pipelines; Final Rule, Federal Register, Vol. 74, No. 232, December, 2009.
6. GPTC Guide for Gas Transmission and Distribution Piping Systems, the Gas Piping Technology Committee, GPTC Z380.1, ANSI Report No. ANSI-GPTC-Z380-TR-1, 2009.
7. Esri ArcGIS Gas Distribution Model http://www.esri.com/industries/gas/business/gas_distribution
8. Spatial Risk Analyst, New Century Software http://www.newcenturysoftware.com/products/spatial_risk_analyst.html
9. Opvantek Optimain DS, Gas Industry Solutions http://www.opvantek.com/solutions/index.html
10. Distribution Risk Assessment Models (DRAM), Report Number S-52-2, GL Noble Denton, to Gas Technology Institute, September, 2011.
11. Natural Disaster Study, National Pipeline Risk Index, Technical Report, U.S. DOT PHMSA, July 1996, https://www.npms.phmsa.dot.gov/data/data_natdis.htm
12. Federal Emergency Management Agency (FEMA), Flood Map Service Center, https://msc.fema.gov/portal
13. U.S. DOT, PHMSA, Cast Iron Inventory, http://opsweb.phmsa.dot.gov/pipeline_replacement/cast_iron_inventory.asp
14. Cast Iron Pipes, http://www.puretechltd.com/types_of_pipe/cast_iron_pipe.shtml
15. O'Rourke, M.J., El Hmadi, K. (1988), "Analysis of continuous buried pipelines for seismic wave effects", Earthquake Engineering and Structural Dynamics, Vol. 16, No. 6.
16. Evaluating Service Life of Anaerobic Joint Sealing Products and Techniques, Cornell University, for Gas Research Institute, Report GRI-96/0318, 1996.

17. British Gas Corporation, "Anaerobic Type Joint Penetrating Systems for Joint Repair on Ferrous Distribution Systems Operating Up to 2 Bar", BGC/PS/LC12, November 1988.

18. Guidelines for the Seismic Design and Assessment of Natural Gas and Liquid Hydrocarbon, Pipeline Research Council International Inc. (PRCI), Project PR-268-9823, 2004.

19. Pipeline Integrity for Ground Movement Hazards, Pipeline Research Council International Inc. (PRCI), Catalog No. L52291, December 2008.

20. Guidelines for Constructing Natural Gas Liquid Hydrocarbon Pipelines through Areas Prone to Landslides and Subsidence Hazards, Pipeline Research Council International Inc. (PRCI), January 2009.

21. ASCE Committee on Gas and Liquid Fuel Lifelines, Guidelines for the Seismic Design of Oil and Gas Pipeline Systems, 1984.

22. ASME B31.8, Gas Transmission and Distribution Piping Systems, American Society of Mechanical Engineers, 2003.

23. Extended Model for Pipe Soil Interaction, Pipeline Research Council International Inc. (PRCI), Catalog No. L51990, August 2003.

24. Guidelines for the Design of Buried Steel Pipe, American Lifelines Alliance (ALA), American Society of Civil Engineers, July, 2001.

25. PIPLIN, Computer Program for Stress and Deformation Analysis of Pipelines, Version 4.59, SSD Inc., December 2013.

26. Specification for Line Pipe, Upstream Segment, American Petroleum Institute (API), API, Specification 5L, 2004

27. Handbook of PE Pipes, Plastics Pipes Institute, Chapter 5, Second Edition, 2012.

28. ASM Specialty Handbook, Cast Irons, ASM International, 1999.

29. Preventing Pipeline Failures In Areas of Soil Movement – Part 1, State of The Art, Pipeline Research Council International Inc. (PRCI), Catalog No. L51516e, 1986.

30. Limit State Function for Excessive Strains in Pipelines Due to Ground Movement, Gas Technology Institute, GRI Report No. GRI-04/0243, March 2005.

31. AgenaRisk User Manual, version 6.2, 2014.

32. Web Soil Survey, U.S. Department of Agriculture (USDA),

   http://websoilsurvey.nrcs.usda.gov/app/HomePage.htm

33. FEMA Modeling Task Force (MOTF)-Hurricane Sandy Impact Analysis, 2015

   https://www.arcgis.com/home/item.html?id=307dd522499d4a44a33d7296a5da5ea0

34. Zhang, K., Chen, S. C., Whitman, D., Shyu, M. L., Yan, J., & Zhang, C. (2003). A progressive morphological filter for removing nonground measurements from airborne LIDAR data. Geoscience and Remote Sensing, IEEE Transactions on, 41(4), 872-882.

35. Girardeau-Montaut, D., Roux, M., Marc, R., & Thibault, G. (2005). Change detection on points cloud data acquired with a ground laser scanner. International Archives of Photogrammetry, Remote Sensing and Spatial Information Sciences, 36(part 3), W19.

36. Kang, Z., & Lu, Z. (2011, January). The change detection of building models using epochs of terrestrial point clouds. In Multi-Platform/Multi-Sensor Remote Sensing and Mapping (M2RSM), 2011 International Workshop on (pp. 1-6). IEEE.

37. Monserrat, O., & Crosetto, M. (2008). Deformation measurement using terrestrial laser scanning data and least squares 3D surface matching. ISPRS Journal of Photogrammetry and Remote Sensing, 63(1), 142-154.

38. Fischler, M. A., & Bolles, R. C. (1981). Random sample consensus: a paradigm for model fitting with applications to image analysis and automated cartography. Communications of the ACM, 24(6), 381-395.

39. Kashani, A. G. and Graettinger, A. J. (2015) "Cluster-Based Roof Covering Damage Detection in Ground-Based Lidar Data" Automation in Construction, 58:19-27.

40. Kashani, A. G., Olsen, M. J., and Graettinger, A. J. (2015) "Laser Scanning Intensity Analysis for Automated Building Wind Damage Detection" 2015 International Workshop of Computing in Civil Engineering, pp. 199-205.